

Control-Oriented Modelling of Wind Direction Variability

Scott Dallas¹, Adam Stock², and Edward Hart³

¹Wind and Marine Energy Systems and Structures, Department of Electrical and Electronic Engineering, University of Strathclyde, Glasgow, United Kingdom

²Institute of Mechanical, Processes and Energy Engineering, School of Engineering and Physical Sciences, Heriot-Watt University, Edinburgh, United Kingdom

³Wind Energy and Control Centre, Department of Electrical and Electronic Engineering, University of Strathclyde, Glasgow, United Kingdom

Correspondence: Scott Dallas (scott.dallas@strath.ac.uk)

Abstract. Wind direction variability significantly affects the performance and life-time of wind turbines and wind farms. Accurately modelling wind direction variability and understanding the effects of yaw misalignment are critical towards designing better wind turbine yaw and wind farm flow controllers. This review focuses on control-oriented modelling of wind direction variability, which is an approach that aims to capture the dynamics of wind direction variability for improving controller performance over a complete set of farm flow scenarios, performing iterative controller development, and/or achieving real-time closed-loop model-based feedback control. The review covers various modelling techniques, including large eddy simulations (LES), data-driven empirical models, and machine learning models, as well as different approaches to data collection and pre-processing. The review also discusses the different challenges in modelling wind direction variability, such as data quality and availability, model uncertainty, and the trade-off between accuracy and computational cost. The review concludes with a discussion of the critical challenges which need to be overcome in control-oriented modelling of wind direction variability, including the use of both high and low-fidelity models.

1 Introduction

Present day large scale wind farms contain arrays of ever increasing numbers of multi-megawatt turbines, with total capacities in the order of gigawatts. The largest wind farm project in the world, under construction in Gansu Province China, will contain around 7,000 turbines and is planned to have a capacity of 20 GW over an approximate area of 500 km squared. The continued increase in the size of wind farms as well as in the size of wind turbines themselves, has resulted in greater interactions between turbines and their surrounding flow fields. These interactions are driven by both large scale atmospheric effects, such as topographically generated weather systems, and more local effects, such as those due to terrain and the wakes of other turbines (Meyers et al., 2022). These complex interactions within the wind farm result in high levels of wind farm performance uncertainty that can lead to under-performance, threatening the viability of wind power to meet the expectations of future renewable energy targets (Haupt et al., 2017).

Active yaw control (yawing the turbine rotor to face against the incoming wind) and wind farm flow control (using control systems to reduce wake effects on downstream turbines) has motivated research into wind direction variability by the wind

energy community. General wind field variability is present in Gaussian wind fields simulated via the turbulence models recommended by IEC 61400-1, the Mann and Kaimal models (Yassin et al., 2021). Direction variation in these models is seen through the argument of the resultant velocity vector of the lateral and longitudinal components. Although useful for fatigue load calculations, research has tended to focus solely on the high frequency wind field content approximated by these models at turbine locations (Dong et al., 2021). Therefore, there is limited understanding of the physical and statistical nature of wind direction variation on length and time scales important for yaw and wind farm flow control (in the order of metres to kilometres and seconds to minutes). Furthermore, the behaviour of wind turbines and wind farms under realistic wind direction variation remains understudied (Shapiro et al., 2022).

This review presents the current understanding of wind direction variability in the context of control-oriented modelling of wind turbines and wind farms in a manner suitable to a wide audience. In doing so, essential gaps in the literature are highlighted and areas in need of further research are made clear. The review is motivated partly by the fact that persistent significant unintentional yaw misalignment (yaw error) of horizontal axis wind turbines (HAWT) with respect to the inflow direction, of more than 10° , is common in many wind farms (Annoni et al., 2019a). ~~This amount of persistent misalignment would result~~ The adoption of wind farm flow control also entails a similar degree of intentional yaw misalignment (Simley et al., 2020b). Whether intentional or not, this degree of persistent misalignment results in a conservative decrease in annual energy production (AEP) of more than $\approx 3\%$ ~~(Pedersen et al., 2008), alongside a corresponding increase in wind energy of the individual turbine~~ (Pedersen et al., 2008), with a corresponding knock on effect to the levelised cost of energy (LCOE) of wind power. AEP aside, there are also the implications of asymmetric loading through turbine components, which could cause increased operation and maintenance costs, further increasing the LCOE (Bartl et al., 2018). Research is ongoing as to the full extent of yaw misalignment on turbine performance and a lack of consensus prevails in the literature, however there are obvious performance implications.

The review begins in Section 2, where the physical drivers of wind field variability at different length and time scales are presented and discussed. Section 3 then outlines the various physical and statistical models used to understand wind direction variability across wind farms over the length and time scales relevant for yaw and wind farm flow control. Next, Section 4 gives an overview of the performance implications of yaw misalignment, both in terms of power and loads. The review then moves on to the topic of control, starting with Section 5 which details conventional yaw controllers and their associated errors and uncertainties. This is followed by Section 6, where methods that augment the control system to improve sensor quality and reliability including methods which utilise machine learning are described. Section 7 then explores two wind farm control methods affected by wind direction variability, namely wake steering control and collective yaw control. Finally, in Section 8, the critical challenges of control-oriented modelling of wind direction variability are summarised and, in Section 9, the conclusions are drawn.

55 2 Physics of Direction Variability

Early research towards understanding dynamic wind direction behaviour began in the field of atmospheric science. Researchers were focused on understanding and predicting the dispersion of pollutants in the atmosphere (Davies and Thomson, 1999). It was found that wind direction variability came in either the form of gradual meandering of the wind vector (Kristensen et al., 1981; Hanna, 1983; Etling, 1990) or frequent sudden changes in direction (Mahrt, 2008). The behaviour was also found to be
60 very closely related to concurrent meteorological and physical conditions, such as the ambient wind speed, the atmospheric stability, local topography, pressure and turbulent motion (Kau et al., 1982). In the wind energy community, wind direction is often treated as a categorical variable (Simley et al., 2020a), or as a conditional variable for direction-dependent coefficient estimation (Feijóo and Villanueva, 2017). In reality, wind direction is a continuous variable with a strong auto-correlation structure (Vincent, 2010), where slight changes can have significant affects on wind farm performance (Porté-Agel et al.,
65 2013). Understanding how wind direction varies over the relevant length and time scales for yaw and wind farm flow control is therefore essential to quantifying performance and achieving control objectives.

Firstly, Section 2.1 gives an overview of the physical processes which cause general inflow variability at wind farms, as well as providing a brief introduction to important terminology from atmospheric science. Next, in Section 2.2, some of the relevant processes in the study of wind direction variability are highlighted and the modelling of these processes is further explored.

70 2.1 Physical Processes

Wind farms experience an array of weather phenomena, resulting in fluctuations in the wind field at different spatial and temporal scales. A subset of meteorological processes and where they fall on the length and time scale is shown in Figure 1.

The largest scale, the synoptic scale, covers atmospheric changes at horizontal length scales in the order of 1,000 km and above, and time scales of approximately one month. The dominant influence on the development of phenomena at the synoptic
75 scale arises from the Coriolis acceleration affecting the movement of air masses (Coleman and Law, 2015). Synoptic-scale processes are mostly relevant for long-term wind energy resource assessment studies (Spera, 1994).

The next largest scale is the mesoscale. Mesoscale meteorology is the study of atmospheric phenomena characterised by horizontal scales in the order of 1 km to 1000 km. Time scales at this level cover less than a day to several weeks. The phenomena often of most interest encompass thunderstorms, fronts, and topography/terrain driven weather systems such as
80 mountain waves (Coleman and Law, 2015). Mesoscale processes influence the location choice and long term operation of wind farms as well as driving smaller scale processes which can affect wind farm performance directly (Spera, 1994).

Lastly, the microscale encapsulates atmospheric phenomena on the smallest scales. These phenomena generally occur over time scales of seconds to minutes and length scales in the order of 1 km or less. This scale focuses on individual thunderstorms, clouds, and local turbulence arising from structures like buildings and obstacles such as individual hills (Coleman and Law,
85 2015). Microscale processes affect the everyday operating environment of wind farms, ~~as they lead to turbine~~. They produce inflow variability on short time scales which can negatively impact performance. These negative impacts are what time scales

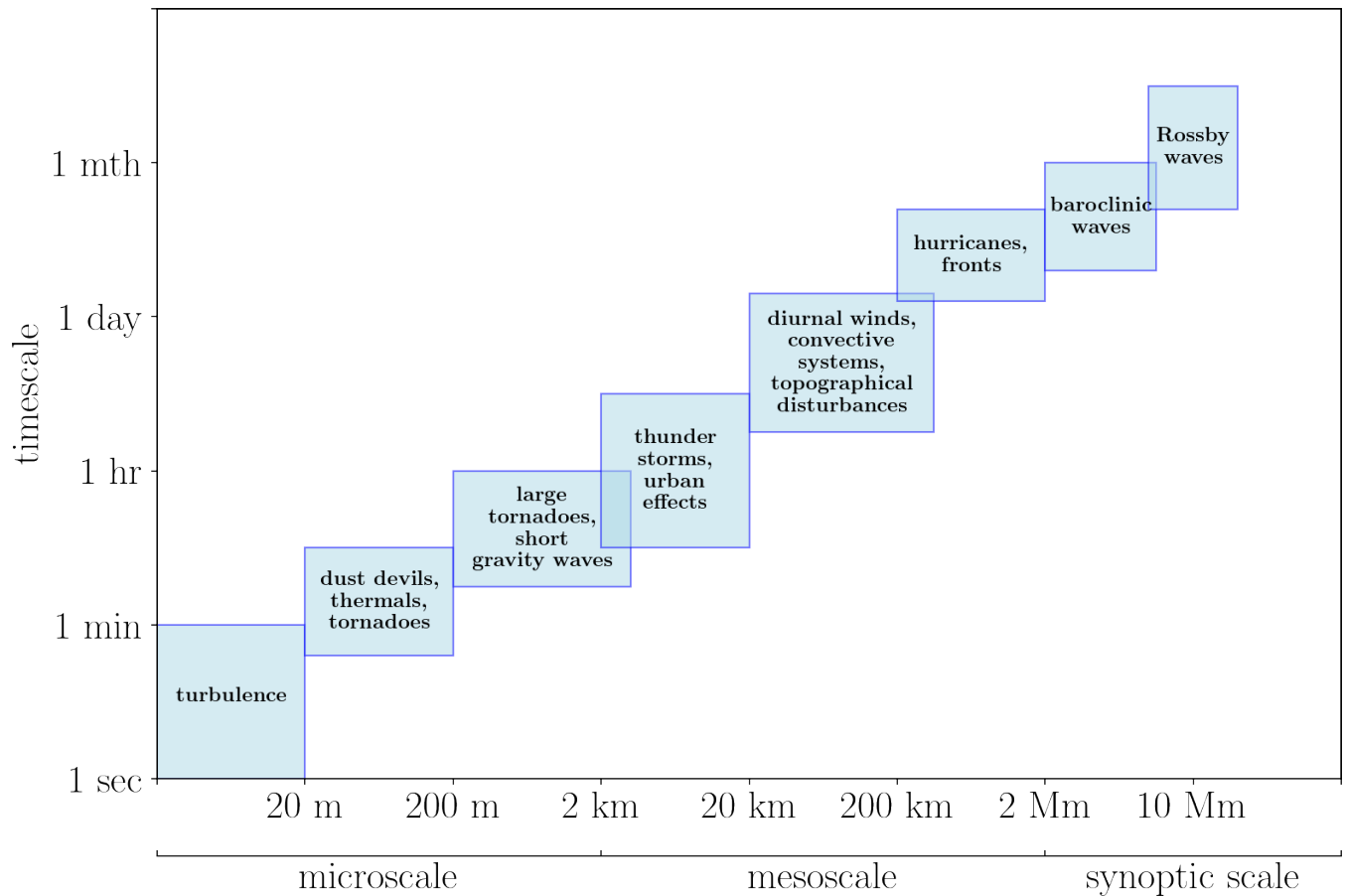


Figure 1. Scales of atmospheric motion and example phenomena.

[similar to the controller response time, which can have a significant impact on performance if not properly accounted for by the yaw or wind farm flow control systems are designed to mitigate system](#) (Haupt et al., 2015).

Many of the microscale processes that occur are so transient in nature that the deterministic description and forecasting of each individual deviation from the general flow of the fluid (eddy) is almost impossible. As a result, there are three primary areas of research regarding the characterisation of eddies (Stull, 1988), which are

- **Stochastic methods** which deal with the empirical average statistical properties of the eddies, these are often studied through simulations using Reynolds-averaged Navier–Stokes (RANS) equations (Section 3).
- **Similarity theory** which describes the apparent common-behaviour of many empirically-observed phenomena, when transformed to the relevant scale. Similarity theory has been applied to wind farm flow data to determine inputs to RANS equations (Breedt et al., 2018).

- **Phenomenological classifications** which inform a partially deterministic approach towards the larger sized eddy structures, these are often studied through large eddy simulation (LES) (Section 3).

2.2 Wind Direction Variability

100 The variability of the wind direction depends highly on the inverse of the wind speed and the stability conditions of the atmospheric boundary layer (ABL). The ABL is the lowest part of the Earth's atmosphere, which directly interacts with the Earth's surface. The height of the ABL depends on various factors such as weather conditions and the time of day. The behaviour of the ABL is often described through its stability condition, which is categorised by three main cases: highly turbulent (unstable), nearly laminar and intermittent (stable), or a combination of the two (neutral) (Meyers et al., 2022).

105 On both the microscale and mesoscale, different sets of dynamics can dominate depending on the ABL conditions, which can have significant effects on wind direction variability and wind farm performance (Meyers et al., 2022). In an unstable atmosphere, ~~small-scale~~ microscale convective processes are of most importance in determining the variability of the wind direction (Vincent et al., 2010). This variability is well understood through ABL similarity theory of turbulence (Hans and Jhon, 1984). On the contrary, in a stable atmosphere, larger ~~scale~~ mesoscale processes are able to exist, such as inertial oscillations, 110 low-level jets, gravity waves and Kelvin-Helmholtz instability, which tend to dominate the variability (Stull, 1988).

Application of traditional similarity theory under stable conditions predicts a reduction in direction variations as stability increases. However, as a consequence of low frequency meanders (Hanna, 1983), this was shown to fail for averaging times of more than 10 minutes (Davies and Thomson, 1999). Low frequency meandering has been attributed to boundary-layer motion and larger mesoscale effects (Hanna, 1983). Low-frequency meanders have been found to exist over all types of terrain ~~and~~ 115 ~~even over~~ including the open ocean, ~~and various~~ Various formulas for estimating such effects have been proposed (Hanna, 1983, 1990; Joffre and Laurila, 1988).

In addition to slow meandering motion, the wind is known to abruptly change direction as well. The underlying mechanics of sudden local wind direction changes remain poorly understood, but potential factors include steepening gravity waves, density currents, pulses of drainage flow, and numerous other more complex phenomena that are difficult to model and predict (Mahrt, 120 2011).

Another crucial aspect is the correlation between wind direction variability and the inverse of wind speed (Joffre and Laurila, 1988; Davies and Thomson, 1999). On average, wind direction variability tends to be higher for unstable conditions at a given wind speed. However, very low wind speeds occur more commonly in stable conditions. As a result, the wind direction variability is generally much larger at night because of the relatively shallow and stable nocturnal boundary layer (Mahrt, 2011). 125 During the late night is also when wind veer (the ~~clockwise~~ rotation of wind direction with height) is especially pronounced as a result of Coriolis forces on the nocturnal boundary layer (Porté-Agel et al., 2020).

The inverse relationship between wind direction variability and wind speed has been successfully modelled and generalised (Joffre and Laurila, 1988; Hanna, 1990). The models help account for wind direction variability with increasing height and between different atmospheric stability classes (Mahrt, 2011). These generalised models have limited application in wind farm

130 flow modelling, since they tend to focus on regimes with very low wind speeds (and therefore high wind direction variability) when most turbines would not be operating.

Finally, terrain effects are also known to impact wind direction variability. In mesoscale simulations, direction variability was found to be greater in complex terrain compared to smoother terrain over small averaging times (in the order of minutes) and showed high sensitivity to the grid point-points selected to represent the on-ground conditions (Jiménez and Dudhia, 2013).
135 Nevertheless, this distinction becomes indiscernible for averaging periods of more than 10 minutes, ~~suggesting that~~. Therefore, local complex terrain predominantly induces greater wind direction variability on shorter time scales, but still significant for yaw and wind farm flow control in the order of minutes or less. Although not sustained, these variations could still have a significant effect on turbine performance if their magnitude is large enough and they last long enough to trigger a control response (see Section 5 for more details on the yaw control system) (Mahrt, 2011).

140 2.3 Discussion of Physics of Direction Variability

The overall drivers of wind direction variability at wind farms is a combination of large scale effects at the synoptic or mesoscale as well as local effects at the microscale (Vincent, 2010). Over longer time periods of several hours (in both stable and unstable conditions) synoptic and mesoscale eddies are the main contributors to wind direction variability (Davies and Thomson, 1999). Certain variation occurs regularly and follows predictable patterns, such as that arising from diurnal and seasonal cycles. Other
145 variations are more sporadic, driven by large-scale weather systems that can induce abrupt changes in wind speed and direction (Haupt et al., 2019). On the other hand, at the microscale, aspects such as atmospheric stability, terrain effects and wake effects are the main drivers of variability.

Each of the drivers of wind direction variability exist on different length and time scales meaning that the statistical properties of wind direction measurements constantly change. Even on very long time scales, climate change ensures that there is no
150 time scale on which the measurements can definitely be considered stationary, meaning that the associated data has means, variances, and co-variances that constantly change over time (Vincent, 2010). Non-stationarity makes it difficult to use physical phenomena as indicators to inform and adjust the parameters of the control system, however, atmospheric stability dependent readjustment time of yaw control parameters has been tested (Cortina et al., 2017).

Fundamentally, there may not be one single direction associated with the wind flowing into large wind farms, especially
155 for those surrounded by complex terrain (Quick et al., 2020). The challenge therefore is to understand how wind direction measurements need to be first filtered and conditioned, before optimisation for control objectives can occur (Hau, 2013). The degree of filtering and conditioning needed will in general depend on other factors such as the concurrent wind speed and atmospheric stability, alongside other site-specific factors like topography, terrain and the specifications of the yaw system itself.

160 3 Wind Farm Flow Models

Wind farm flow models are mathematical, statistical and/or computational models used to simulate and analyse the behaviour of wind flow within wind farms. Many different flow models exist that take into account various different global and/or local effects, however, they have traditionally been developed by various research communities in isolation (Sanz Rodrigo et al., 2017). Recently, attempts have been made to bridge the gaps, especially between the fields of atmospheric physics, statistics and fluid dynamics, where collaboration is motivated by the need for realistic inflow conditions in high fidelity wind farm flow studies (Chatterjee et al., 2018).

One question is whether or not a sufficient picture of the relevant physics can be captured by wind farm flow models, such that they can be used for controller testing and validation in a reliable and accurate way. ~~Current developments in high fidelity farm flow models~~, accurate and cost-effective manner. Recent developments in LES models with concurrent mesoscale precursor simulations would allow for such ~~simulations-tests~~ to be performed, although ~~at great still at considerable~~ computational expense. Thus, the ~~number of processors-amount of computational resource~~ required to achieve useful results using these ~~high fidelity-LES~~ models is out of reach to the majority of the researcher community.

Section 3.1 discusses ~~the current~~ physical models that have incorporated realistic dynamic wind direction changes as input and briefly describes how they work. Section 3.2 then follows with discussion of the statistical tools and models that have been applied to the study of wind direction variability over the relevant length and time scales.

3.1 Physical Models

Physical models used in wind farm flow simulations fall into one of three broad categories; high fidelity large eddy simulations (LES), medium fidelity dynamic models or reduced order (engineering) models.

- **High fidelity LES models** are the most accurate but still computationally feasible microscale farm flow simulation tools available. Instead of ~~direct numerical simulations~~ prohibitively expensive direct numerical simulation of the Navier-Stokes equations of fluid dynamics, LES works by filtering out the smallest length-scales of the Navier-Stokes equations (the smallest eddies). Generally, LES is used to simulate statistically stationary behaviour of wind farms, however, realistic dynamic wind direction variation can be included by coupling LES with mesoscale forcings that prescribe the wind farm inflow through precursor simulation methods (Section 3.1.2) (Munters et al., 2016).
- **Medium fidelity dynamical models** can be employed to predict the available power and/or flow fields in a wind farm (Boersma, 2019). These equations often use Reynold’s averaged Navier-Stokes (RANS) equations based models, which, unlike LES, represent only the mean fluid flow. RANS models mostly consider steady-state behaviour, but models can be adapted to analyse preset changes in wind farm conditions over space and time, such as continuous sweeps across inflow directions (Kheirabadi and Nagamune, 2021).
- **Reduced-order or engineering models** can provide information on important wind farm dynamics with limited computational complexity (Boersma, 2019) which give typical run-times in the order of seconds to minutes, useful for iterative

controller design. However, these models are valid for only specific atmospheric conditions, don't contain any true turbulent eddy structure and have limited accuracy (Schreiber et al., 2020).

LES models are the highest fidelity models available and have been used successfully for testing new wind farm flow controllers (Storey et al., 2016; Gebraad et al., 2016). The quality of these models are constantly being improved by validation against and assimilation of field test data, as well as recent attempts to couple them with mesoscale precursor models (Munters et al., 2016; Chatterjee et al., 2018; Stieren et al., 2021). However, the grid points needed to resolve a developed stratified wake with LES is in the order of 1×10^{11} , according to conservative estimates (Li et al., 2022). Hence, the computational cost is prohibitively expensive for most controller design purposes, not to mention the cost associated with the wind turbine aero-elastic models required to gain a complete picture (Larsen et al., 2017). Therefore, LES is not suitable for most control-oriented modelling applications. Instead, LES often serves as a proof-of-concept tool for new control methods or as validation models for lower-order surrogate models (Meyers et al., 2022).

The best available models for understanding the effects of wind direction variability are coupled mesoscale-microscale LES models. Although, again these models are unsuitable for most control-oriented modelling applications, they are able to simulate farm wide realistic dynamic changes in inflow direction and have provided valuable insights. Therefore, Sections 3.1.1 and 3.1.2 describe in more detail mesoscale, microscale and coupled models and introduce examples from the literature.

3.1.1 Mesoscale and Microscale Models

Mesoscale models of wind farms include physical parameterisations to model the outer flow phenomena by including energy transform models, surface layer models, land use models, physical parameterisation, boundary layer parameterisations, and more. By incorporating suitable initial and boundary conditions derived from global models, these models effectively capture the dynamic processes of the ABL (Haupt et al., 2019). These important dynamics are often excluded from or only roughly approximated in more local LES (microscale) models. Furthermore, mesoscale models are non-hydrostatic and model water-related processes in the atmosphere, both rare features of microscale models. Although realistic wind direction variability can be captured using mesoscale models (Draxl et al., 2021), the maximum horizontal-spatial and temporal resolution of these models is too large to allow them to accurately investigate intra-wind farm effects caused by dynamic wind direction changes (Carvalho et al., 2012; Jiménez and Dudhia, 2013), however, they are useful in studying general wind farm flow effects such as inter-wind farm wakes and the development of wind farm boundary layers.

In contrast to mesoscale models, microscale LES models, have the ability to capture the flow around objects at much higher resolution, allowing modelling of terrain details and flow around turbine blades (Haupt et al., 2020). These models are also able to resolve fine-scale turbulence and explicitly resolve aeroelastic interactions with the wind turbines. Microscale LES models, therefore, are essential towards developing new optimal yaw and wind farm flow control strategies (Fleming et al., 2014a, 2015). However, up to now the emphasis has been on small-scale turbulence modelling and scenarios where the farm flow is constrained towards steady-state conditions (Calaf et al., 2010; Wu and Porté-Agel, 2011; Goit et al., 2016). While these simulations have offered valuable insights into the interaction of wind farms and the ABL under steady-state conditions,

225 the influence of large-scale effects on wind farm performance, especially dynamic wind direction changes, has mostly been ignored (Stieren et al., 2021).

3.1.2 Coupled Models

There have been efforts to accurately couple mesoscale models to microscale LES (Muñoz-Esparza et al., 2014; Muñoz-Esparza and Kosović, 2018; Haupt et al., 2020), which is particularly important to accurately represent non-stationary meteorological
230 conditions or changes of atmospheric stability at wind farms, especially those driven by the diurnal cycle (Haupt et al., 2020). For coupled simulations, Coriolis effects are included which means large changes in wind direction with height in the ABL can be simulated (Haupt et al., 2017). Therefore, in order to represent a wider range of important meteorological phenomena that affect wind farm performance, mesoscale information needs to be embedded in microscale models (Draxl et al., 2021).

Realistic inflow conditions from mesoscale forcing can be included in microscale LES by nesting the LES within a mesoscale
235 numerical weather prediction (NWP) simulation domain. The output of the NWP acts as a precursor to the LES simulation, providing both the initial and boundary conditions. Examples include coupling LES to mesoscale models like the Weather Research and Forecasting (WRF) model (Talbot et al., 2012; Mirocha et al., 2014; Schalkwijk et al., 2015). Biases in wind speed and direction in nested mesoscale simulations have been shown to be passed on to the LES simulations, which in general are unable to fully correct for these biases (Talbot et al., 2012). However, the wind field is reasonably well simulated by the
240 WRF model, especially in wind regimes where there is a very dominant sector (Carvalho et al., 2012), and can be improved with appropriate data assimilation techniques (Haupt et al., 2017).

The goal of accounting for realistic dynamic wind direction or even sweeps over a range of predetermined wind directions in LES is challenging and demands significant computational resource. To this end, a concurrent precursor method in which the horizontally periodic mesoscale precursor domain was rotated was first proposed by Munters et al. (2016). Following up on
245 this work, Chatterjee et al. (2018) proposed a modified version of the concurrent method that only rotated the inflow velocity vector instead of the entire precursor domain. Data from cup and vane anemometer was used to generate realistic neutral ABL inflow data to the modified model to compare the predicted wake effects with on-site light detection and ranging (LiDAR) measurements of the wakes (Chatterjee et al., 2018). The approach has since been developed further by Stieren et al. (2021) to make use of a dynamically changing non-inertial rotating reference frame, which was able to accurately reproduce realistic
250 pseudo-random wind direction and power spectrum at each turbine using low-pass filtered wind farm field measurements as inputs.

The coupled LES models provide greater understanding of how dynamic wind direction changes can significantly impact wind farm performance. As an example, simulations of a regularly spaced wind farm array demonstrated a considerably steeper decline in power output at the minimum farm power inflow angle, θ_{min} (the wind direction at which lowest wind farm power
255 output occurs), during a dynamic wind direction sweep compared to what was predicted through a series of static simulations at various but constant inflow directions (Munters et al., 2016; Stieren et al., 2021). The drop in power was explained by the high-velocity wind speed channels which exist between turbines. The flow in these channels was much stronger during static simulations at θ_{min} compared to simulations which considered a sweep over directions, where channel flow is disrupted by

the inflow angle, especially between turbines further downstream (Stieren et al., 2021). The effect was less pronounced for low
260 wind direction rotation rates, since the channel flow had enough time to speed up and allow the entrainment of energy from the
channels into the waked region (Munters et al., 2016). This effect also produced a spike in wind farm power at wind farm flow
angles far away from θ_{min} . It also was shown to cause a site specific hysteresis effect, detected as a positive or negative shift
in the value of θ_{min} of the wind farm (Munters et al., 2016; Stieren et al., 2021).

3.2 Statistical Models

265 Statistical models are useful as inputs to wind farm simulations in order to account for and accurately reflect uncertainty in
the inflow conditions. Since wind direction is fundamentally non-stationary, this necessitates simplifying assumptions and
approximations about the statistical nature of wind direction time series so they can be more easily modelled. In general,
there is a relative lack of research focusing on the statistics of wind direction as opposed to wind speed (Jiménez and Dudhia,
2013), especially in the context of wind farm flow, which seems to be a product of the challenges associated with the statistical
270 treatment of circular variables like wind direction (Mardia et al., 2000). Often in studies, the longitudinal and latitudinal
components of the wind vector are shown instead of the wind direction, which avoids the difficulties associated with summary
statistics of circular data (Haupt et al., 2017).

Therefore, one critical question is how to treat the circular wind direction variable. In contrast to linear statistics, there are
often different ways to calculate summary statistics of circular data, such as the sample mean for instance, which in most
275 cases give different results. Therefore, careful consideration of the appropriate circular statistics is needed, before making any
calculations (Farrugia and Micallef, 2017).

3.2.1 Circular Statistics

Circular statistics deal with data that has a circular or directional nature, where the values need to be measured in terms
of a circular scale. In contrast to traditional linear statistics, where values can be measured with respect to the real number
280 line, circular statistics takes into account the wrapping of the variable, where any value beyond the maximum or minimum
are wrapped back on the scale, creating distributions that exist on the circle rather than the real number line. Wind direction
provides a good example of a circular variable. It is 2π periodic and can be mapped to a circular scale where an arbitrary
zero-direction and manner of rotation are defined (Jammalamadaka and SenGupta, 2001). Conventionally, the zero-direction
is set as north and then angles are measured clockwise from [therenorth](#).

285 The periodicity of circular variables, the arbitrariness of the zero position and manner of rotation, and the absence of absolute
magnitude, altogether means directional analysis of circular data is substantially different from standard linear statistical anal-
ysis. Circular statistical methods need to be invariant with respect to the choice of the zero-direction and sense of rotation, as
a consequence, many typical linear techniques and measures are not applicable. Therefore commonly used summary statistics,
such as the [sample](#)-mean and variance, as well as simple mathematical operations like subtraction and addition, need to be
290 redefined so they make sense in the context of circular statistics (Jammalamadaka and SenGupta, 2001).

Before the circular mean and variance can be discussed further, the absolute minimum angular distance $|\Delta(\theta_1, \theta_2)|$ needs to be defined. This quantity gives the absolute value of the least angular distance between two angles (represented by θ_1 and θ_2 here), and is defined as,

$$|\Delta(\theta_1, \theta_2)| = \min(|\theta_2 - \theta_1| \bmod 2\pi, 2\pi - |\theta_2 - \theta_1| \bmod 2\pi).$$

295 The associated sign of the minimum angular distance $\Delta(\theta_1, \theta_2)$ depends on the choice of the zero-direction and the sense of rotation (Farrugia et al., 2009).

The minimum angular distance is needed to compute the expected values of essential summary statistics, like the circular mean and standard deviation (Yamartino, 1984; Farrugia et al., 2009). The circular mean $\bar{\theta}$ and circular variance $\sigma_{\bar{\theta}}^2 v_R$ of a sample of N circular variables $\{\theta_i\}_{i=1}^N$ can be obtained in a variety of ways. The most intuitive easiest to visualise is the vectorial method and involves which begins by representing the circular data as a set of unit vectors in the complex plane $\{z_i\}_{i=1}^N$, where $z_i = e^{i\theta_i}$. The circular mean is then calculated as the argument of the resultant vector z_R after summation of the unit vectors.

$$\bar{\theta} = \arg\left(\frac{1}{N} \sum_{i=1}^N z_i\right) = \arg(z_R). \quad (1)$$

Figure 2 illustrates calculation of the circular mean of two different sets of circular variables. Note that for wind data, calculation of the circular mean can also be weighted by the corresponding wind speed V_i in order to capture more information about the wind field.

Once the circular mean $\bar{\theta}$ is obtained, the circular variance $\sigma_{\bar{\theta}}^2 v_R$ can then be calculated according to,

$$\sigma_{\bar{\theta}}^2 v_R = \frac{1}{N} \sum_i \Delta_i^2 - \frac{1}{N} \sum_i \Delta_i^2 \bar{R}, \quad (2)$$

310 where $\Delta_i = \Delta(\theta_i, \bar{\theta})$. This quantity is of particular interest since the standard deviation of $\bar{R} = |z_R|$ and $0 \leq \bar{R} \leq 1$. Since the length of the resultant vector \bar{R} decreases as the spread of the data around the circle, $1 - \bar{R}$ increases with the spread and therefore provides a robust measure of the variance (Fisher, 1995). One limitation of this measure is that it is bounded between 0 and 1, which makes it difficult to interpret in the same way as the equivalent value in linear statistics.

If the data is known to lie within a narrow range of values (which is almost guaranteed for wind direction time series in the order of tens of minutes), the use of linear statistics to calculate the variance as well as other summary statistics becomes valid¹ (Rott et al., 2018). Before linear summary statistics can be calculated, the minimum angular distance $\Delta(\theta_1, \theta_2)$ needs to be defined. This quantity gives the signed value of the least angular distance between two angles (represented here by $\theta_1, \theta_2 \in [0, 2\pi)$), once the zero-direction and sense of rotation have been defined. There exists different examples in the

¹Otherwise, if the dataset contains values more than π radians away from the circular mean, calculating variance in the linear sense isn't well defined since it is unclear what the difference between those extreme values and the mean should be.

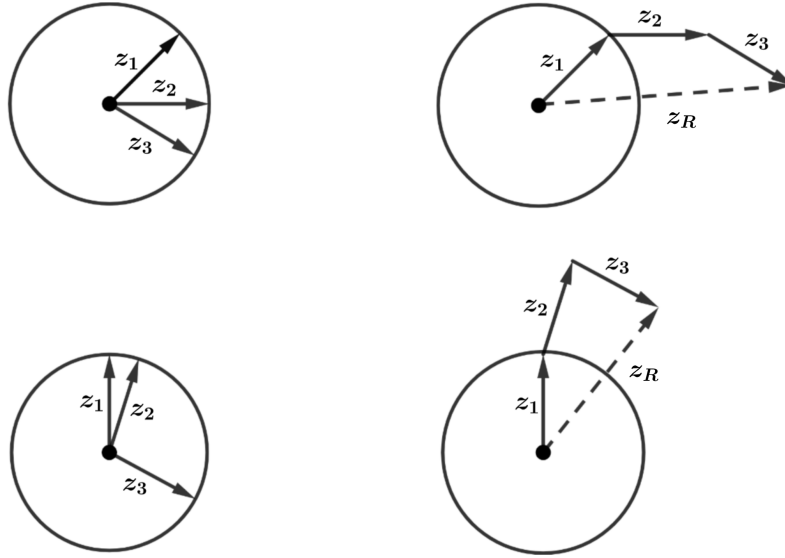


Figure 2. Examples of circular variables represented as unit vectors in the complex plane $\{z_i\}_{i=1}^3$ and resultant vectors z_R indicated by dashed lines. The circular mean is then the argument of the resultant vector in each case. Adapted-Illustration adapted from Cremers and Klugkist (2018).

literature of how to calculate this quantity, the first $\Delta_{Farr}(\theta_1, \theta_2)$ comes from Farrugia et al. (2009) where the authors start
 320 by defining the absolute minimum angular distance as

$$|\Delta_{Farr}(\theta_1, \theta_2)| := \min(|\theta_2 - \theta_1| \bmod 2\pi, 2\pi - (|\theta_2 - \theta_1| \bmod 2\pi)). \quad (3)$$

The minimum angular distance is then determined by considering a series of cases concerning the relative position of each
 angle on the circle and assigning a sign to the absolute value accordingly. However, this approach does not account for all cases
 and therefore is incomplete. A complete and succinct definition is given in Rott et al. (2018), where the minimum angular
 325 distance $\Delta_{Rott}(\theta_1, \theta_2) \in [-\pi, \pi]$ is simply given by,

$$\Delta_{Rott}(\theta_1, \theta_2) := ((\theta_2 - \theta_1 + \pi) \bmod 2\pi) - \pi, \quad (4)$$

from which the absolute value can easily be determined if necessary.

The minimum angular distance is used to compute the expected values of linear summary statistics such as the standard
 deviation and the variance (Yamartino, 1984; Farrugia et al., 2009). The variance σ_θ^2 can be computed according to,

$$330 \quad \sigma_\theta^2 = \frac{1}{N} \sum_i \Delta(\bar{\theta}, \theta_i)^2 \quad (5)$$

where $\Delta(\bar{\theta}, \theta_i)$ is the distance from the mean according to the chosen measure of the minimum angular distance. The standard
 deviation of wind direction σ_θ is of particular interest to researchers since it is related to the lateral turbulence intensity i_v
 through the equation $\tan(\sigma_\theta) = i_v$ in stable atmospheric conditions (Hanna, 1983).

3.2.2 Short Term Statistical Models

335 In order to quantify variability for robust wake steering control, where upstream turbines operate with an intentional yaw
misalignment to deflect their wakes away from those downstream (Simley et al., 2021), statistics of 5 minute wind direction
time series have been studied from one second wind vane met mast data (Rott et al., 2018). The measurement data was
split into 5 minute time series, mapped to a linear scale, and compared with a fitted normal distribution both visually, using
histograms and quantile-quantile plots, and numerically, using a Kolmogorov–Smirnov test. The comparison was done to verify
340 the hypothesis that the measurement data can be approximated statistically by a normal distribution within 5 minute segments.
It was found that 70.58% of the measurements passed the test for a significance level of 5%. Based on these findings, it was
concluded that in the majority of cases, the variability of 5 minute wind direction time series can be adequately approximated
by a normal distribution. It was also verified that wind direction variability is strongly correlated with atmospheric stability
classes, as discussed in Section 2, which included stable, neutral and unstable conditions (Rott et al., 2018).

345 Similarly, it has also been shown that a normal distribution provided a good fit to the measured wind direction variations
over a longer 10 minute time period at Horns Rev (Gaumond et al., 2014). The wind direction measurements were recorded
using a sonic anemometer mounted on a met mast with a sampling rate of 12 Hz at a height of 50 meters (Peña and Hahmann,
2012). The assumption that the wind direction time series was normally distributed over the considered sampling times meant
that the yaw **misalignment**-errors at each turbine could be assumed to be normally distributed as well, which allowed power
350 performance to be more accurately calculated. Hence, the accuracy of three separate wake models was evaluated against data
from the Horns Rev wind farm while taking into account uncertainty in the wind direction measurements.

Alternative data driven methods for modelling and generating realistic short term wind field time series samples have also
been described (Bossanyi, 2018; Simley et al., 2020a; Van Der Hoek et al., 2021). Bossanyi (2018) started from single-point
measured data, which were 10-minute averages of wind speed, direction and standard deviation from a met mast. To preserve
355 the correct 10-minute statistics, smooth time-series were fitted to the points and synthetic turbulence was then added. While
the wind field included all three components of turbulence, the lateral component was zero-mean, therefore dynamic changes
in inflow wind direction were subsequently added from the smoothed met mast data.

Alternatively, both Simley et al. (2020a) and Van Der Hoek et al. (2021) modelled the wind direction by generating different
stochastic time series which represented either the slowly varying mean wind direction across the wind farm or the purely
360 turbulent high frequency component with zero mean. The time series were produced by simulating a random time series with a
normal distribution, derived from the power spectra of both low-frequency and turbulent wind direction components extracted
from met mast measurements and LES. This method resulted in time series where the low frequency wind direction components
were completely correlated at each turbine whereas the high frequency components were completed uncorrelated.

Strong assumptions are made by these data driven models, especially in how wind direction changes propagate through the
365 farm, however, data-driven methods are designed to minimise computation requirements and act only as a starting point to be
iterated and refined upon. Other, more general wind field generation techniques are also available and widely used, such as

the Mann spectral model (Mann, 1998) or the Veers method (Veers, 1988), however, these methods focus mostly on modelling stationary processes and the high frequency content of the wind field.

3.3 Discussion of Wind Farm Flow Models

370 Meso-microscale coupled LES models have the potential to validate a controllers effectiveness under realistic wind direction variability before more detailed field tests are carried out (Section 3.1.2). However, the computing power required by current models makes them prohibitively expensive and time consuming to deploy, especially for complex control optimisation (Munters et al., 2016; Stieren et al., 2021).

Ideally, software would allow many multiple 5 to 10 minute wind farm flow simulations to test controller effectiveness under dynamic wind changes, enough to achieve statistical significance. Although current data-driven methods make strong assumptions about wind direction, especially in terms of normality of time series and their spatial and temporal coherence, the short-term statistical treatment of the wind direction variable presented in Section 3.2 provides a starting point for a data-driven, computationally less expensive approach to the problem.

4 Performance under Yaw Misalignment

380 Yaw misalignment, denoted γ_E , refers to any misalignment between the rotor axis with nacelle position $\theta_{nacelle}$ and the hub height wind direction θ_{wind} . Figure 3 shows the top down view of a turbine with positive yaw misalignment.

The misalignment is calculated according to

$$\gamma_E = \Delta_{Rott}(\theta_{nacelle}, \theta_{wind}) \quad (6)$$

where $\theta_{nacelle}$ and θ_{wind} may each be either time-averaged or instantaneous, depending on the application.

385 There are two classes of yaw misalignment; intentional, because of the actions of a wake steering controller (or simply because of the necessarily slow actuation of the yaw system), or unintentional, because of systematic measurement bias or other errors in the wind turbine measurement equipment.

This section starts by providing motivation for the topic through the physical laws that govern horizontal axis wind turbines. Section 4.1 covers the first-order relationship between power and yaw misalignment of the wind turbine. Then, Section 4.2 gives a brief overview of the current understanding of the effects of yaw misalignment on turbine loads.

4.1 Power

From the continuity equation of fluid mechanics, the flow of an air mass $\frac{dm}{dt}$ is a function of air density ρ , surface area (in this case the rotor swept area) A_r , and free stream flow velocity U_∞ . Ignoring the effects of wind shear and veer, it is estimated that the velocity is independent of location on the rotor swept area, meaning that $\frac{dm}{dt}$ through the rotor can be defined as,

$$395 \quad \frac{dm}{dt} = \rho A_r U_\infty. \quad (7)$$

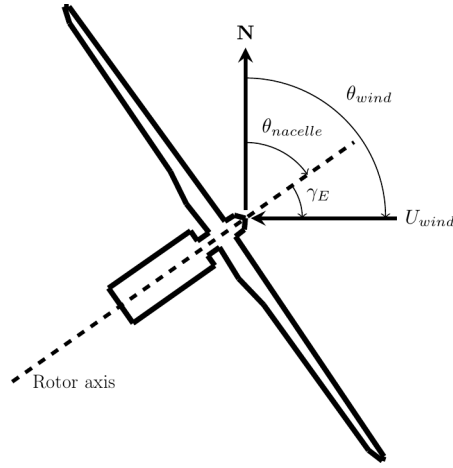


Figure 3. Positive yaw misalignment $\gamma_E = \theta_{wind} - \theta_{nacelle}$ on a horizontal axis wind turbine which is defined as a counter clockwise rotation of the rotor nacelle away from the hub height wind direction viewed from above. Adapted Illustration adapted from Fleming et al. (2016).

The instantaneous kinetic power of the wind available at the rotor, P_w , is

$$P_w = \frac{1}{2} \frac{dm}{dt} U_{wind}^2 = \frac{1}{2} \rho A_r U_{\infty}^3. \quad (8)$$

A wind turbine exerts a thrust force F on the wind flowing through the rotor that corresponds to the amount of energy extracted from the flow each second,

$$400 \quad F = \frac{1}{2} C_T(\beta, \lambda, \gamma) \rho A_r U_{wind}^2, \quad (9)$$

where U_{wind} is the free-stream wind velocity after taking into account induction effects and $C_T(\beta, \lambda, \gamma)$ is the dimensionless thrust force coefficient, which is a function of the blade pitch β , tip-speed ratio λ , and yaw angle γ . The tip-speed ratio is defined as the ratio of the tangential speed at the blade tip to free-stream wind velocity,

$$\lambda = \frac{\omega R}{U_{\infty}}, \quad (10)$$

405 where R is the radius and ω is the rotational speed. The tip-speed ratio is proportional to the rotor speed, which is typically controlled via the generator torque or by pitching the turbine blades to alter the lift forces on them (Boersma et al., 2017). The power in the wind across a circular cross section was given in eq. 8 but not all of this power can be extracted by a wind turbine. The wind power that can be extracted by a turbine is given by,

$$P = \frac{1}{2} C_P(\beta, \lambda, \gamma) \rho A_r U_{wind}^3, \quad (11)$$

410 where $C_P(\beta, \lambda, \gamma)$ is the dimensionless power coefficient (Boersma et al., 2017).

The theoretically maximum available power at any given wind speed occurs when the rotor axis is aligned to the inflow wind direction. If the rotor axis of a turbine is not aligned with the inflow, the wind speed perpendicular to the rotor plane is reduced to

$$U_{\gamma_E} = U_{wind} \cos(\gamma_E), \quad (12)$$

415 where γ_E is the yaw misalignment of the turbine. Hence, neglecting changes in aerodynamic behaviour from misaligned rotors, the maximum amount of power that can be extracted by a turbine operating with a yaw error γ_E is

$$P_{max} = \frac{1}{2} \rho A_r U_{wind}^3 \cos^3(\gamma_E) C_p. \quad (13)$$

Thus, the extractable power is theoretically reduced by a factor of $\cos^3(\gamma_E)$. In reality, experimental results have shown that power extraction under yaw error behaves according to the more general empirical equation,

$$420 \quad P_{max} = \frac{1}{2} \rho A_r U_{wind}^3 \cos^\alpha(\gamma_E) C_p, \quad (14)$$

where the term $\cos^\alpha(\gamma_E)$ is referred to as the power reduction factor (PRF). The α term has been estimated both experimentally and theoretically in several different studies, which are discussed in Section 4.1.1.

4.1.1 Power Reduction Factor

Experiments carried out using a rotating wind turbine model in a wind tunnel with turbulent inflow generated by a static grid
425 found that the empirical value of the power reduction factor mostly agreed with the expected value, i.e. $\alpha \approx 3$ (Krogstad and Adaramola, 2012). A similar set up with low and high turbulence uniform inflow and sheared inflow condition also found that $\alpha \approx 3$ (Bartl et al., 2018). However, other experimental results have often shown that the cube law overestimates the power loss (Kragh and Hansen, 2015). An overview of past research and their findings is shown in Table 1.

Turbine Model	α Value	Paper
Scale model	≈ 3	(Krogstad and Adaramola, 2012; Bartl et al., 2018)
Scale model	≈ 2	(Medici, 2005)
NREL 5MW LES model	1.88	(Gebraad et al., 2014)
Scale Model	≈ 1.7870	(Schreiber et al., 2017)
Scale model, LES model	$\approx 1.43, \approx 1.43$	(Draper et al., 2018)
Envision 4MW turbine, LES model	$\approx 1.86, \approx 1.73$	(Fleming et al., 2017)
Various OEM models	≈ 2	(Howland et al., 2020)

Table 1. Selected details of past research and findings for the power reduction factor $\cos^\alpha(\gamma_E)$.

In addition to the empirical observations outlined in Table 1, Howland et al. (2020) developed a model from first principles,
430 using blade element momentum (BEM) theory to show how there exists a non-linear relationship between power output and

yaw misalignment, affected by both the atmospheric conditions and the wind turbine control system. The data collected to test their model showed $\alpha = 2$ for different OEM turbines at a specific site. It was concluded that the ability of the first principles model to accurately predict performance was much greater than the simple cosine cubed power law, since the expected power will in all cases be model- and site-specific. [Additionally, Heck et al. \(2023\) used a similar first principles approach to understand how not only the power, but the induction, thrust and near wake velocity deficit changed in relation to yaw misalignment. This approach showed that induction decreases as a function of yaw misalignment, which explains the less than expected value of \$\alpha\$ observed in various studies \(Table 1\).](#)

4.2 Loads

Fatigue loading occurs when a load is repeatedly applied and removed from a material, i.e. when the loading is cyclic. For wind turbines, cyclic loads usually occur as the blade rotates through a wind field, leading to what is called once-per-revolution (1P) loads on the blade and 3P loads on the tower and drivetrain (Kragh and Fleming, 2012). The effects of yaw misalignment on turbine component and structural fatigue loads as well as lifespan changes is somewhat of an open question (Bartl et al., 2018).

A misaligned inflow produces periodic loads because the aerodynamics of the blade change with its azimuthal position θ . The advancing and retreating action of the blade with respect to the crosswind flow creates a change in the angle of attack, leading to changes in the lift, drag and thrust forces (Heck et al., 2023). The changes in thrust force combine to create a moment on the rotor in the tilt direction. Figure 4 shows a free body diagram of a blade element before and after applying a positive yaw misalignment. As the blade passes through $\theta = 0$ and $\theta = \pi$, the effect of the misalignment is at a minimum since it is cancelled by the blade position, whereas the effect is maximal at $\theta = \pi/2$ and $\theta = 3\pi/2$. Additional periodic loading occurs because of a slow down in the turbine's wake on one side compared to the other, which results in increased forces on the blade during that portion of the rotation (Zalkind and Pao, 2016).

Damage equivalent load (DEL) is the single equivalent load at some fixed frequency that produces the same amount of damage as the actual loading history. The distribution of DELs and extreme loads under yaw misalignment for various degrees of yaw misalignment have been found to be rather complex but correlated with the rotor and blade design as well as the ambient wind conditions (Damiani et al., 2018). These load distributions were measured for a fully instrumented wind turbine and compared to predictions from an aeroelastic model, where it was found that the model predicted the distributions well (Damiani et al., 2018). Modelling deficiencies in other aeroelastic models and complex unsteady-flow phenomena during yaw were also revealed by comparison of load characteristics on a misaligned model turbine rotor to various computational approaches (Schepers et al., 2014).

More recently, it was shown [how that](#) the DELs are not distributed symmetrically around the zero misalignment angle on the turbine's main bearings (Cardaun et al., 2019). In fact, it was found that [rotating the rotor to the right of the top down rotation of the rotor clockwise with respect to the](#) inflow lead to smaller loads in general. This effect has since been attributed to the rotor tilt, which, at $\gamma_E = 0$, results in a minor increase in the effective wind speed on one side of the rotor while reducing it slightly on the other side (Hart et al., 2022). Similarly, the yaw moments on misaligned rotors were observed to increase approximately

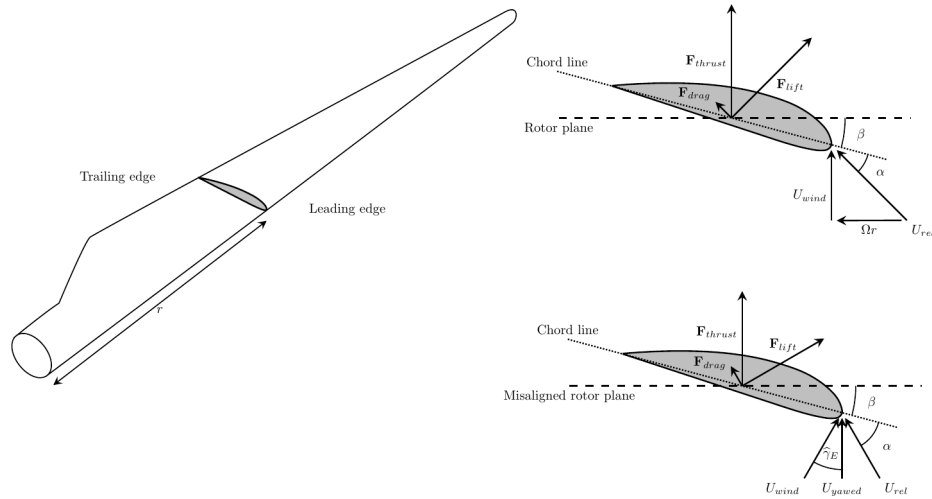


Figure 4. Blade element dynamics under normal and yawed conditions, $\hat{\gamma}_E = \gamma_E \sin(\theta)$ and $U_{yawed} = U_{wind} \cos(\hat{\gamma}_E)$. [Adapted Illustration adapted](#) from Howland et al. (2020).

linearly with increasing degrees of yaw misalignment but again the moments were not completely symmetrically distributed
 465 around the zero misalignment angle (Bartl et al., 2018).

It has been argued that the effects of yaw misalignment can be balanced by wind shear, such that there exists a turbulence-intensity dependent optimal non-zero yaw misalignment angle which minimises blade loads (Kragh and Hansen, 2014; Damiani et al., 2018). However, the reduction in blade loads at this angle were shown to be accompanied by an increase in load fluctuations for other components, such as the drivetrain and tower (Kragh and Hansen, 2014; Zalkind and Pao, 2016).

470 4.3 Discussion of Performance under Yaw misalignment

The performance effects due to misalignment between the rotor and the inflow wind direction are complex and dependent on a number of factors including the turbine model and the ambient wind conditions.

Levels of yaw misalignment greater than 10 degrees are not an uncommon occurrence according to the literature (Pedersen et al., 2008, 2011; Kragh and Fleming, 2012; Annoni et al., 2019a). Figure 5 highlights typical mean and maximal misalignment
 475 angles as well as power losses expected at different values of power reduction factor. From Figure 5, it can be seen that commonly found levels of yaw misalignment in the literature can cause anywhere from an $\approx 1.5\%$ to $\approx 4.5\%$ decrease in AEP.

Yaw misalignment also causes asymmetric loading through the blades and rotor, leading to increased wear and tear on the components of the turbine, reducing their lifespan and increasing maintenance costs, with knock on effects on LCOE (Section 4.2). Although the blade loads under yaw misalignment have been well described and verified in multiple studies,
 480 more understanding of the aerodynamics of yaw misalignment is still required, including differences between positive and negative misalignment angles, as well as how the rotor is affected by both vertical and horizontal variations in direction (Howland et al., 2020).

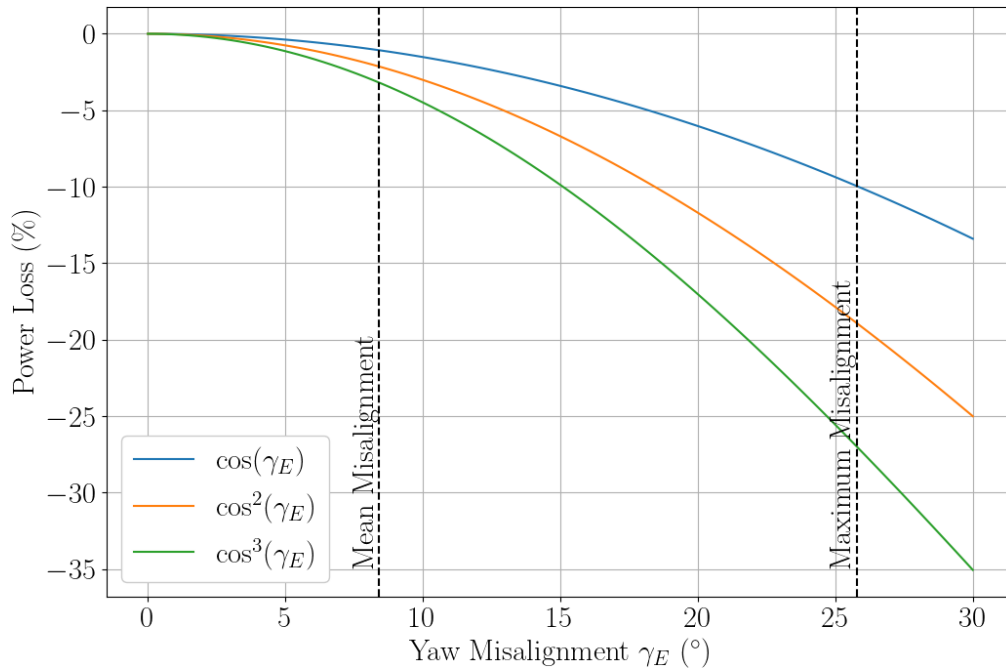


Figure 5. Power loss against misalignment for different power reduction factors with typical mean and maximal yaw misalignment values indicated from data presented by Annoni et al. (2019a).

The first order approximation of yaw misaligned rotor dynamics (Figure 4) provide a good starting point in understanding site and atmosphere specific effects of yaw misalignment on power and loads (Howland et al., 2020). Then, if these dynamics are integrated into aero-elastic turbine simulations, control-oriented models could be developed with these dynamics in place, resulting in better understanding of the efficacy of control actions to minimise the deleterious effects of yaw misalignment.

5 Conventional Yaw Control

The rotational movement of the wind turbine rotor around the axis of the turbine tower is the yaw of the turbine (Kragh et al., 2013b). Yaw controllers are designed to align the wind turbine rotor axis with the hub height wind direction as best as possible, while balancing the constraints of the system (Meyers et al., 2022). As discussed in Section 4, the wind turbine’s yaw system can have significant effects on overall wind turbine performance in terms of both power and loads.

It is important to note that the control architecture of commercial wind turbines is often proprietary and dependent on the manufacturer, and so information on the operation of conventional wind turbine yaw systems is only available to a limited extent in the literature. The discussions in this section, therefore, may not be true for all wind turbines but they do serve as motivation for further discussions on alternatives to conventional yaw systems.

This section begins by describing the architecture of conventional yaw control systems in Section 5.1. Then, the common errors and uncertainties associated with conventional wind direction measurement instruments are discussed in Sections 5.2 and 5.3 respectively.

5.1 Architecture

500 The majority of modern utility-scale horizontal axis wind turbines use an active yaw drive mechanism to face the turbine into the wind. An estimate of current wind direction is the first step in most yaw systems. Traditionally, a wind vane on top of the nacelle measures the wind direction at a point behind the rotor plane. The wind direction signal is usually measured at high frequency by the wind vane (Bossanyi, 2019). The wind direction signal is then passed through a heavy low-pass filter, which smooths out the short-term variations, makes the resulting signal more representative of rotor-averaged variations and

505 ensures the yaw system depends only on the relatively low-frequency changes in the wind direction. As an example, a first-order low-pass filter with a -3 dB cut-off frequency of 2 mHz was applied to the input wind direction in CFD simulations of yaw control (Gebraad et al., 2016). The filtered signal is then compared with the nacelle orientation to obtain a measure of yaw misalignment. An example of typical conventional yaw control architecture is shown in figure 6 (Chen et al., 2020).

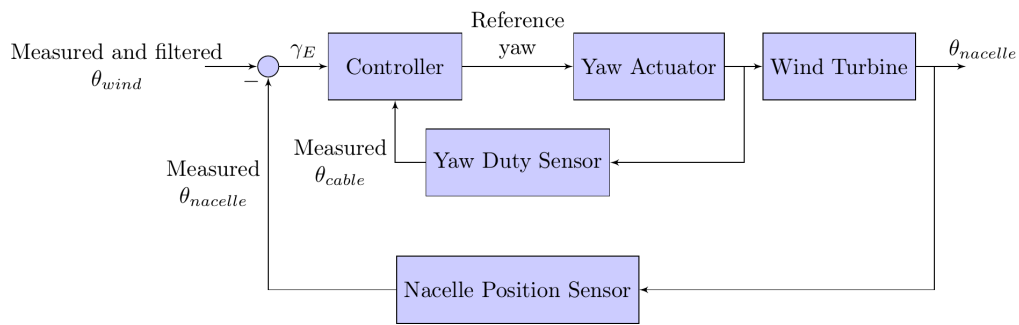


Figure 6. Schematic of a typical conventional yaw system. The yaw duty sensor measures cable rotation θ_{cable} to ensure the rotation remains within safe limits. [Adapted-Illustration adapted](#) from Chen et al. (2020).

In addition to low-pass filtering, a hysteresis dead-band, effectively a buffer zone where no control action is taken, is introduced to prevent frequent yaw manoeuvres and avoid dangerous gyroscopic forces. This avoids what is known as ‘yaw hunting’, where the yaw controller tries to follow the time-varying wind direction too closely without allowing for an amount of variability and uncertainty in the signal. If the turbine were to yaw at such a high rate, this would have negative consequences on the lifetime of the yaw system as well as the loads on other components. Most large turbines yaw at rates of less than 1 deg/s (Pao and Johnson, 2009) and the controller is typically only activated when the yaw error measured by the wind vane

515 exceeds some threshold (Spencer et al., 2013). An example from the literature comes from the baseline controller from the pre-design phase of the DOWEC 6MW turbine (Kooijman et al., 2003). This controller used a 30 second moving average of the wind direction to monitor yaw misalignment. The controller activated yaw actuators when the yaw error reached 5 degrees

with a yaw rate of 0.3 degrees per second until the 2 second moving average of yaw error was less than 0.5 degrees (Storey et al., 2016).

520 Due to the constraints described, the yaw system is in standstill most of the time (Kim and Dalhoff, 2014). It is typical for the yaw angle to remain constant for about 5 to 10 minutes before the yaw control corrects for the changes in wind direction and reduces the yaw misalignment (Rott et al., 2018). The contrast between the slowly reacting yaw systems of modern utility-scale wind turbines and the variability of the wind direction signal is a product of the trade off between minimising yaw duty and yaw hunting while at the same instance maximising turbine performance.

525 5.2 Measurement Errors

Wind vanes or sonic anemometers positioned atop the nacelle within the disturbed flow region behind the rotor are often used to measure the apparent hub height wind direction (Kragh et al., 2013a). On-site met masts are sometimes also available to provide measurements, however it is more convenient in general to use measurements from instruments on the turbines themselves. Each turbine control system can provide a hub height wind direction estimate by comparing the measured nacelle
530 position against the input low-pass filtered yaw misalignment signal, which all relies heavily on correct calibration of the instrumentation (Bossanyi and Ruisi, 2021).

Measurements taken by sensors positioned behind the rotor on the nacelle, within the disturbed flow, have been shown to be significantly affected by flow distortions caused by the rotor (Kragh and Fleming, 2012). Computational fluid dynamics (CFD) simulations of the flow distortions around the nacelle revealed a strong sensitivity of the wind direction measurement
535 to the position of the sensor on the nacelle (Zahle and Sørensen, 2011). It was revealed that the nacelle flow angles exhibited substantial variations with height above the nacelle surface. The CFD simulations showed that the flow was primarily governed by unsteady vortex shedding from the cylindrical part of the blades connected with the rotor hub interacting with the root vortices from each of the blades, resulting in the creation of significant velocity gradients. The effect of flow distortion has also been shown in field studies. Nacelle mounted sensors showed significant dependence of flow distortion on both yaw and
540 tilt angles with yaw error of up to 10 degrees when operating in a tilted inflow (Zahle and Sørensen, 2011). Additionally, analysis of operational data from a V80 2 MW onshore turbine revealed below-rated mean yaw errors of 10° (Pedersen et al., 2008, 2011), whereas separate analysis of the CART3 600 kW research turbine showed rotor speed-dependent mean yaw errors of 5° to 15° (Kragh et al., 2013a).

Further inaccuracies can be introduced purely from the way the yaw control system is set up and operated. Firstly, for the
545 Horns Rev I wind farm, analysis of operational data showed the yaw signals to be mostly wrong when turbines were not operating (Draxl, 2012). Upon restart, with the turbine yawed at a random angle, it took time for the sensor to be oriented correctly again, resulting in a period of inaccurate data (Draxl, 2012). Secondly, complications common to many wind turbines were introduced by the turbines' own cables, which had to be disentangled after too much rotation around the yaw axis, meaning the turbine had to be rotated back and then re-adjusted against the other sensors again (Draxl, 2012). Lastly, an EU
550 project (UpWind) found that the wind vane signals of both onshore and offshore turbines were often not correctly calibrated, with neighbouring turbines measuring substantial differences in yaw alignment (Eecen et al., 2011).

Biases in turbine wind direction signal can be corrected once they have been identified. For example, a speed-dependent linear regression correction scheme, based on empirical data, was applied to a yaw controller input signal (Kragh et al., 2013a). With the correction applied, the new yaw control architecture was able to reduce yaw errors compared to the baseline controller. However, the relatively short amount of data available meant the findings could not be properly substantiated, and precluded any additional conclusions about load reductions.

5.3 Measurement Uncertainty

An important issue highlighted, especially in wake steering research, is the wind direction uncertainty present in data sets (Gaumont et al., 2014; Rott et al., 2018; Simley et al., 2020a; Campagnolo et al., 2020). This uncertainty is guaranteed due to the stochastic behaviour of the wind. The uncertainty can also be exaggerated through standard methods of time averaging as well as from spatial interpolation, as a result of the natural variability of the wind direction and the distance from the reference location to where the measurement is taken.

Operational data sets are often binned by wind direction sectors in order to simplify the calculation of other important variables, mainly power production. However, the accuracy of wind farm flow models was found to heavily depend on the width of the wind direction sectors used for binning the simulation results (Gaumont et al., 2012). Hence, over narrow wind direction sectors, differences between the power outputs predicted by wind farm flow simulations and real wind farm power output data sets are potentially caused by the large wind direction uncertainty in the data sets, and not because of modelling deficiencies (Gaumont et al., 2012). As a result, there is now a recognition of the need to incorporate uncertainty into wind farm flow models to produce better and more robust controllers.

In order to quantify uncertainty in wake models and to design better wake steering controllers, the distribution of high-frequency wind direction measurements within 5-minute (Rott et al., 2018) or 10-minute (Gaumont et al., 2014) windows was approximated using a Gaussian probability density function. By quantifying uncertainty, deficiencies in wake modelling were identified and inflow specific adaptations to wake steering controllers were explored.

Similar approaches inspired by the Gaussian distribution approximation of the wind direction have also been developed. For example, the yaw position uncertainty was included in wake steering set-point calculations alongside the wind direction uncertainty as a joint Gaussian distribution where the sums of the variance of each equalled the variance of the yaw error (Simley et al., 2020a). Another approach used polynomial chaos expansion to account for uncertainties while optimising for wake steering set-points which included a Laplace distribution for the yaw misalignment and a Gaussian distribution for the wind direction measurement (Quick et al., 2020). The polynomial expansion approach revealed that uncertainty in the wind direction measurement had one of the largest impacts on the set-point optimisation results, highlighting the importance of understanding wind direction variability for both yaw and wake steering control.

5.4 Discussion of Conventional Yaw control

Control based on conventional sensing methods mainly suffers from two factors. The first is the significant noise, uncertainty and outliers in the inputted wind direction measurement. These problems have been found to be due to a mixture of the

585 placement of the sensing equipment, the inadequacies of standard measurement instruments and the intrinsic complexity of
the wind direction variable (Kragh and Fleming, 2012; Kragh et al., 2013a). Secondly, the slow actuation of the yaw system,
although necessary to avoid negative gyroscopic forces, results in turbines operating misaligned most of the time (Mikkelsen
et al., 2010). The misalignment can be significant, especially when a wind direction change happens rapidly and abruptly
before the yaw system has time to respond.

590 Control parameters of conventional systems are often determined through a trial and error approach (Bossanyi, 2019), which
in many cases is sub-optimal and prone to the proliferation of bias (Mikkelsen et al., 2010) (Section 5.2). In most cases, biases
can be identified and corrected using simple detection and correction algorithms (Kragh et al., 2013a). The uncertainties,
however, are less easily handled, especially those arising from natural variation in the wind direction. One proposed solution
is to use an optimisation under uncertainty methodology for robust control, which entails the incorporation of the uncertainties
595 into the calculation of control parameters and set points (Section 5.3).

6 Alternative Yaw Control

Research to improve yaw control has focused on alternative sensing or data-processing methods that provide more accurate
inputs to the control system and/or provide a preview of wind direction changes before they occur at the turbine. Alternatives
can be broadly categorised by how their input signal is obtained; measurement-free, inferred, forecasted, based on improved
600 measurement equipment, or estimated. It is important to note that some of these methods can be complimentary to each
other. For instance, estimation techniques can be used to further enhance control based on remote sensing. The categories are
described as follows,

- 605 – **Measurement-free yaw control** originates from early wind turbine ~~research design, which was~~ limited by the ~~measurement
and control~~ technology of the time. ~~The~~ It has since been investigated as a means to avoid the reliance on potentially
erroneous measurements of the wind direction (Farret et al., 2001; Xin et al., 2012; Karakasis et al., 2016). The suggested
mechanism of this set of controllers is to directly search for the maximum power point without a wind direction
input signal (Farret et al., 2001; Xin et al., 2012; Karakasis et al., 2016). For example, Karakasis et al. (2016) used the
difference between optimal rotor speed and actual rotor speed to track the real-time performance of turbines and adjusted
the yaw set-point accordingly.
- 610 – **Inferred signal based yaw control** is where measurements of other closely related variables are used to infer the wind
direction and yaw misalignment angle. For example, an estimation of the yaw misalignment in the below rated domain
can be calculated from an inverted function of wind power and wind speed (Tsioumas et al., 2017), or from the rotor
angular speed (Karami et al., 2021), and then incorporated into the control system with the appropriate architecture.
Nacelle-mounted anemometer wind speed measurements are less affected than the wind vane by flow distortions caused
615 by the rotor and are easier to correct for than wind direction measurements at the same location (Smith et al., 2002).
Therefore, the measurement errors and uncertainties associated with wind vane measurements discussed in Section 5
can mostly be avoided without the need for additional sensing equipment.

620 – **Forecasting for yaw control** is where very short term predictions ~~of the time series are calculated in order to preemptively react to any changes~~ (in the order of minutes) of wind direction are calculated to allow the yaw system to pre-emptively react to a forecasted change in wind direction (Section 6.1).

– **Yaw control with additional or alternative sensing** which could replace or augment nacelle mounted wind vanes. The most popular alternatives are remote sensors based on LiDAR and hypersonic (SoDAR) technologies (Barthelmie et al., 2016) (Section 6.2).

625 – **Enhanced signal estimation for yaw control** which involves families of both parametric and non-parametric methods of communication based spatial filtering, bias correction and/or error detection. Some of these methods work by updating the parameters of physics-based models to obtain farm-wide direction estimates, whereas others are purely stats based (Section 6.3).

Since the latter three methods directly address the handling of the wind direction signal (forecasting, improved measurement, and estimation), they are discussed in more detail. Firstly, wind direction forecasting for both yaw control and ~~more general purpose~~ also for more general purposes is discussed in Section 6.1. Next, in Section 6.2, improved measurement methods are 630 discussed that reduce uncertainty in the wind direction signal. Finally, in Section 6.3, an outline of wind direction estimation techniques that can improve the quality of wind direction signals without any additional or improved sensing equipment is given.

6.1 Wind Direction Forecasting

635 Since the statistical properties of the wind field evolve with time (Section 2), the forecasting of wind direction is an especially complex task (Hirata et al., 2008). Non-stationarity necessitates the use of non-parametric methods and adaptive spectral analysis to produce accurate ~~short term forecasts~~ forecasts minutes-ahead. The use of very short term wind ~~field-direction~~ forecasts for control purposes is motivated by the preview effect, where information about incoming changes to the flow field can be used to preemptively carry out a desired control action. Theoretically, accurate short term forecasts could improve 640 turbine yaw performance by reducing the time delay between changes in direction and activation of the yaw system. This is especially attractive in a yaw control setting where response time is limited greatly by the slowness of the yaw actuators.

There are four general categories of methods for forecasting wind direction,

645 – **Persistence methods** assume that the wind direction at time t is the same as at time $t + \Delta t$. Unsurprisingly, the performance of this method is comparable to physical and parametric methods only for very-extremely short term forecasts (Hirata et al., 2008; El-Fouly et al., 2008). This approach is the most naive and is only used as a baseline comparison.

– **Machine learning (ML) and statistical methods** have been used several times to forecast the wind direction variable for wind energy applications. The simplest are regression models (linear or piecewise-linear) (Howland et al., 2022a), Kalman filters (Song et al., 2018) and time series models which include various auto-regressive predictors (Erdem and Shi, 2011; Song et al., 2017). The complex nature of wind direction time-series presents challenges when applying these

650 techniques. Parametric-based forecasters, in particular, tend to be susceptible to bias (Kim, 2003), and although they are easy to implement, most of these methods are linear while wind direction time-series are non-linear in nature (Chitsazan et al., 2019).

- **Numerical weather prediction (NWP)** refers to any physics based approach in meteorological forecasting. NWP models tend to be general-purpose models that can be used for a wide variety of applications including wind direction forecasting. In general, the resolution of NWP models is too coarse to be useful for most wind energy applications, however, one study has demonstrated the performance of an extremely high resolution numerical weather prediction model (Chan and Hon, 2016). A maximum resolution of 200 meters was achieved, but required numerous meteorological instruments and large amounts of processing power, making it poorly suited for yaw or wake steering control-oriented applications.
- **Hybrid methods** make use of mixed models from either statistics or NWP alongside artificial intelligence based methods to improve forecasting. For example, gradient boosting trees ML algorithms were combined with feature engineering techniques to extract the maximum forecasting information from a NWP grid (Andrade and Bessa, 2017). Another example used a circular regression based approach, which was developed alongside a Bayesian averaging method for bias correction of the forecasts obtained by NWP models (Bao et al., 2010).

665 Methods from machine learning and statistics are the most useful for control purposes since they can be implemented at a local level and in real-time, allowing for adaptive adjustments over extremely short time intervals. Therefore, they are discussed further in Section 6.1.1.

6.1.1 Forecasting with Machine Learning and Statistics

Several wind direction forecasting methods based on machine learning for yaw or wake steering control have been investigated, including an auto-regressive integrated moving average (ARIMA) model approach paired with a Kalman filter (KF) (Song et al., 2017). ARIMA models are well-suited for capturing short-term correlations and have been used extensively in a diverse mix of forecasting applications (Fisher and Lee, 1994; Bivona et al., 2011). In general, however, the ARIMA model by itself is unable to adjust its parameters effectively as new time-series information becomes available. To solve the adjustment problem, the ARIMA model was combined with a Kalman filter (KF), which assimilates new data and updates the model's parameters systematically (Su et al., 2014; Song et al., 2018). The ARIMA-KF model was able to predict the one step ahead 10 second mean wind direction with a mean absolute error (MAE) of 0.92° over a 4 hour validation window after assimilating 20 hours of training data. When incorporated into yaw control, the new system was able to recover 1-2% of lost power due to yaw misalignment compared to a baseline conventional controller.

680 A simple linear regression-based method was also used to forecast the wind direction during periods of mean wind direction transitions to produce inputs to various wake steering controllers (Howland et al., 2022a). The linear regression approach resulted in an MAE of 1.3° after a time horizon of 30 minutes during transition periods compared to an MAE of 1.9° when the low-pass filtered wind direction signal was used. More complex forecasting methods from machine learning have also been explored, including four different data mining algorithm prediction approaches (Ouyang et al., 2017). Support vector machines,

neural networks, random forests and gradient boosted regression trees were each trained and tested on a years worth of wind direction data at 10 minute intervals, transformed into cosine and sine components. Although it was found that the methods based on random forests and neural networks performed best at predicting the 10 minute ahead sine and cosine components of the wind direction, performance improvements by integration of forecasts into the yaw system were not demonstrated.

6.2 Improved Sensing Equipment

Various different solutions have been suggested which use advanced sensing equipment to improve the wind direction input signal to the yaw control system. One way is to augment or replace the wind vane with a LiDAR system mounted on the nacelle, on the ground or on the rotating spinner of the turbine to detect the undisturbed wind in front of the turbine over the entire rotor (Mikkelsen et al., 2013; Simley et al., 2014; Fleming et al., 2014b; Scholbrock et al., 2016). By installing a spinner anemometer in front of the rotor, the measurements are likely to be less influenced by rotor-induced flow distortions, offering advantages over measurements obtained from a sensor placed behind the rotor (Kragh et al., 2013a). Simulations demonstrated that a spinner mounted continuous wave LiDAR can estimate yaw misalignment with a median precision below 4° (Kragh et al., 2011). In field tests, good correlation was found between estimates of yaw error determined using a spinner mounted LiDAR and those estimated based on met mast data (Kragh et al., 2013b). Further field tests also demonstrated how a nacelle mounted LiDAR can correct measurements from a nacelle mounted wind vane, resulting in increased yaw alignment and significantly improved power capture compared to the uncorrected baseline case (Fleming et al., 2014b).

Similar to forecasting techniques, LiDAR and other remote sensing methods can allow for further performance gains by providing wind field preview information to the yaw control system. A LiDAR capable of providing preview wind direction information for the next 60 seconds, harnessed using conventional model predictive control (MPC) in the yaw system, could yield an 8% increase in power production and potentially lead to reductions in fatigue loads during instances of extreme wind direction changes (Spencer et al., 2013). Likewise, the performance of a yaw control system with access to preview information from forward facing LiDAR coupled with a long-short term memory neural network was tested against a conventional yaw control system in simulations (Chen et al., 2020). It was found that incorporating preview information could increase power capture by up to 3.5%, reduce yaw travel by up to 5.3%, and reduce yaw events by up to 3.9%.

Other advanced measurement technologies similar to LiDAR have also been tested, namely RaDAR and SoDAR. For example, a spinner anemometer consisting of three SoDAR sensors performed well in field tests (Pedersen et al., 2008), although it is unclear if such devices are commercially available yet. Other improvement techniques involve the use of additional conventional measurement equipment placed strategically around the wind farm in order to better characterise the inflow (Chen et al., 2022).

6.3 Wind Direction Estimation

As discussed in Section 2, the wind direction can vary greatly spatially and temporally due to variable meteorological conditions, local topography and wake effects. Therefore, on top of the possible misalignment biases on local direction measurements discussed in Section 5.2, the direction is often different at different locations in the wind farm. Hence, in a lot of cases, even in

the presence of enough sensors and/or advanced sensors, it is still difficult, if not impossible, to get an accurate global picture of wind direction. Under these conditions, distributed wind direction estimation techniques can be considered.

720 The earliest example explicitly for control purposes was presented by Doekemeijer et al. (2018). A non-linear Kalman filter was used to assimilate data and update the parameters of a medium-fidelity physical wind farm flow model with the objective of achieving real time closed-loop wake steering control. However, only high frequency changes in wind direction were accounted for by the model, such that a constant mean value was assumed over the entire simulation time interval. In order to address lower frequency changes in wind direction, Sinner et al. (2020) used a simpler polynomial based Kalman filter and updated the parameters of the model through the assimilation of SCADA data. The major benefit of this approach is the ability to provide smooth wind direction estimates, even in the case of faulty individual turbine sensors, while only using measurements already
725 collected at the wind turbines.

Non-parametric methods have also been developed to estimate the wind direction. In the work by Annoni et al. (2019a), comparisons were made between different non-parametric approaches for estimating the wind direction at turbine locations. The most accurate of these methods in terms of MAE was a distributed consensus-based optimisation approach. This approach was shown in simulations to reliably estimate the wind direction across a wind farm even when faults and/or biases were
730 introduced in the wind vane signals. The MAE of the consensus-based approach was 2.99° compared to 3.78° for the best averaging based approach, weighted averaging, and 8.41° when using the sensors alone. Additionally, Bossanyi (2019) also investigated weighted averaging methods for improving wind direction estimates. Short 30 minute wind farm simulations showed that these methods improved yaw control performance and by extension wind farm power production compared to using only the turbine's wind vane signal (Bossanyi, 2019).

735 More recently, Van Der Hoek et al. (2021) applied Gaussian process (GP) regression to the problem of wind direction estimation. GP regression is a non-parametric Bayesian approach to regression (Rasmussen, 2003), which can be used not only to estimate the wind direction at any point within the wind farm, but also for bias detection and correction. Thus, the GP approach provided a balance between the qualities of the parametric and non-parametric methods previously described. Van Der Hoek et al. (2021) found that a simple GP model with a squared exponential kernel was able to filter the high-frequency
740 component of artificially generated wind direction data and reproduce the known low-frequency wind direction variation at turbine locations better than standard low-pass filtering. However, there was no discussion around the choice of kernel to calculate the covariance or interpretation of model hyper-parameters, both of which needed further exploration to improve the model's accuracy.

745 It is important to point out that in order to test these estimation techniques, in most cases it was necessary to generate an artificial 'true' wind direction signal as input to the simulations (Section 3.2). This entailed making strong assumptions about the 'true' wind direction, which limits how applicable the results of this section are to real world conditions. Nonetheless, these methods provide an indication of how to best generate realistic and dynamic wind direction changes which could serve as inputs to control-oriented models.

6.4 Discussion of Alternative Yaw Control

750 Errors in measurement of the wind direction at each turbine can be reduced through a variety of alternative and novel methods. The reduction in errors results in overall performance improvements, often without any adaptation or augmentations to the turbines themselves and with minimal alteration to the control architecture.

Forecasting methods, for example, have harnessed the preview effect to preemptively yaw; reducing misalignment errors and improving wake steering controllers (Howland et al., 2022a) (Section 6.1). Similarly, remote sensing equipment such as LiDAR
755 systems have been shown to improve performance through the same effect by measuring the incoming wind some distance in front of the turbine, while also improving wind direction sensing in general (Section 6.2). However, remote sensing technology comes with the added costs of the equipment itself, the expertise needed to operate them effectively and uncertainties in how much turbine performance can be improved by their use (Spencer et al., 2013). Therefore, the relative size and cost of the wind farm needs to be taken into account before making any decisions, since any improvements in performance and reduction in
760 loads may not be substantial enough to justify the extra costs.

Estimation methods such as spatial filtering have been shown in limited simulation scenarios to reduce signal uncertainty and boost overall yaw controller performance without any changes to the actuators or sensing equipment (Bossanyi, 2019; Annoni et al., 2019a; Van Der Hoek et al., 2021) (Section 6.3). Spatial filtering can also make use of the preview effect in downstream turbines by passing information from turbines further upstream (Bossanyi, 2019).

765 Although these results are all promising, it is fundamentally difficult to rigorously characterise the effectiveness of wind direction forecasters, sensors and estimators, particularly due to the difficulties in generating ‘true’ wind direction signals to compare them against. Indirect indicators like power production can be used instead, however these will in general be much more sensitive to the wind speed rather than the wind direction, hence caution needs to be taken when setting benchmarks.

7 Wind Farm Flow Control

770 Wind farm control (WFC) considers the entire wind farm as a control system, with individual turbines acting as agents in a network, helping to achieve farm-level objectives (Sinner et al., 2021). Wind farm flow control (WFFC) is a subfield of WFC where the control objective is achieved through manipulation of the intra-wind farm flow. Two promising developments in the area of WFFC are wake steering control, and communication-based spatial filtering, which aims to enhance the accuracy and reliability of information used by turbine- and farm-level controllers by combining together wind field measurements gathered
775 from individual turbines (Sinner et al., 2021).

This section briefly introduces examples of both wake steering control, in Section 7.1, and communication-based spatial filtering for yaw control (designated as collective yaw control), in Section 7.2. The examples represent a small subset of available control methods but are chosen as they are designed to handle wind direction input variability directly.

7.1 Wake Steering Control

780 Wake steering control provides an example of WFFC sensitive to wind direction changes. Although it can be achieved through
various methods, this section focuses on the the most popular method found in the literature, the use of static yaw misalignment
of upstream turbines. Similar to the objectives of yaw control, in wake steering control, the goal is to balance yawing frequently
785 enough to maintain power maximisation while avoiding overuse of the yawing components (Houck, 2022). Contrary to the
objectives of yaw control, however, upstream turbines are operated with an intentional yaw misalignment to redirect their wakes
away from downstream turbines, therefore mitigating potentially substantial power losses caused by wake effects (Howland
et al., 2019). Wake steering controllers have been shown to result in farm-wide power performance gains in both simulations
and field experiments (Howland et al., 2022b). Results from one field experiment revealed power production gains of up to
14% for a downstream turbine over a 10° wind direction sector (Fleming et al., 2019), however, the total farm wide power
gains (or in some cases losses) from wake steering control are sensitive to atmospheric conditions, local terrain and the specific
790 turbine model (Annoni et al., 2018b; Fleming et al., 2019).

Commercial wake steering controllers are available, an example is the WakeAdaptTM software offered by Siemens Gamesa
(Energy, 2022), but the details of their operation is mostly proprietary. Because of this privacy, there is limited information
available on how the software works in general. In the literature, wake steering controllers solve a dynamic optimisation
problem at the wind farm level in order to identify optimal yaw set-points that manipulate the wind field in such a way
795 that power losses are minimised (Kheirabadi and Nagamune, 2019). These set-points are then tracked by wind turbine level
controllers.

Most wake steering controllers in the literature are designed such that the yaw set-points are optimised under stationary
or steady inflow conditions. This has changed recently by the incorporation of wind field variability into already established
model-based yaw set-point optimisation methods. For example, a steady-state wake model was enhanced by including yaw
800 system deviations from set-point values in the corresponding wake steering yaw set-point calculations (Quick et al., 2017). This
optimisation approach has since been taken a step further such that the set-point calculations were formulated as optimisation
under dynamic wind direction uncertainty, as opposed to static and deterministic inflow (Rott et al., 2018). Furthermore,
methods for set-point optimisation under uncertainty, with special consideration of wake model parameter uncertainty, resulted
in demonstrable improvements for open-loop and closed-loop wake steering control (Howland, 2021).

805 7.1.1 Graph and Cluster View

A simplification of wind farm flow, particularly in regard to control of the turbines whose wakes interact, is the graph or cluster
view of the wind farm. The graph view is an abstraction of the wind farm as a collection of cells, nodes (turbines) and edge
weights between nodes which change depending on the incoming wind direction and wake effects. The cluster view similarly
groups turbines which are coupled through their wakes. Clusters are defined such that the performance of the turbines in each
810 cluster is only significantly affected by the operation of the other turbines in the same cluster.

Examples of graph-based and cluster-based approaches are those developed by Starke et al. (2021) and by Bernardoni et al. (2022) respectively. The graph-based model proposed by Starke et al. (2021) employed edge weights based on inter-turbine wake interaction intensity and time delays to simulate how the effects of wind direction changes propagate through the wind farm. The graph-based approach employed a Gaussian wake model to calculate velocity deficits and the wake profile (Shapiro et al., 2019). In contrast, the cluster-based approach of Bernardoni et al. (2022) was model-free and used only power data to identify wind direction changes and turbines coupled through wake interactions.

Both types of approaches can lead to efficiency improvements in a distributed control setting and reduce some of the computational challenges associated with real-time control applications, as only the relationships between selected turbines are considered rather than the whole farm or velocity field (Bay et al., 2018; Annoni et al., 2018a, 2019b; Bernardoni et al., 2020). An advantage of the graph-based approach over standard wind farm flow modelling approaches is that it can be integrated with a dynamic wind farm flow model which accounts for changes to wind direction through a time-dependent change in the graph structure. This overcomes the difficulty and computational expense of implementing a dynamic wind change in models that have a fixed domain often with a fixed mean wind direction, such as LES, RANS, or data-driven models trained for a single-inlet condition (Shapiro et al., 2022).

Both the graph and cluster-based approaches provide simplifications for identifying and responding to changes in power output due to changes in wind direction. However, these simplifications are significant and have not been thoroughly validated yet. For example, calculating the correct weightings in the graph-based approach relies on knowing the real wind dynamics, which in turn would ideally need LES or similar to validate. Likewise, the model free cluster-based approach relies solely on power data correlated over time windows in the order of tens of minutes, which introduces limitations on how accurately interacting turbines can be identified and how quickly changes in wind direction are detected. To a greater or lesser extent, both approaches are only able to capture mean wind field effects across the wind farm, which limits their ability to quantify uncertainty in their results as well as for use in a robust control framework.

7.2 Collective Yaw Control

Collective yaw control can be achieved through the use of appropriate consensus algorithms for estimating wind conditions at different wind farm locations (Section 6.3). The sharing of data among turbines not only reduces signal noise via spatial filtering (Sinner et al., 2021), it can also help to identify and correct any faults or bias in individual turbine measurements (Annoni et al., 2019a; Van Der Hoek et al., 2021), which not only confers greater control robustness but also extra redundancy against equipment failures. The reduction in noise and error terms through consensus methods means they can be used to improve yaw and wake steering controller performance through collective yaw control. Table 2 outlines past research and selected findings.

The ability of collective yaw control to improve performance was first demonstrated by Bossanyi (2019) and then by Sinner et al. (2021). The most simple wind direction estimation technique, based on averages weighted by distance from nearby turbines, was investigated in both studies. It was found that power production can be improved over short simulation periods

Software Used	Control Method	Consensus Method	Power Gain	Yaw Duty Reduction	Identifies Yaw Bias	Paper
LongSim	CYC	Weighted average	$\approx 0.2\%$	$\approx 24\%$	No	Bossanyi (2019)
FLORIS Version 2.1.1	CYC, CYC + WSC	Weighted average	0.5%, 4.7%	46.1%, 17.0%	No	Sinner et al. (2021)
Custom in-house	CYC	Gaussian processes	NA	$\approx 20\%$	Yes	Van Der Hoek et al. (2021)
Custom in-house	CYC	Distributed optimisation	NA	NA	Yes	Annoni et al. (2019a)

Table 2. Selected details of past research. CYC = Collective Yaw Control, WSC = Wake Steering Control.

845 compared to the use of conventional control methods by up to 0.5% in the case of yaw control alone and 4.7% when combined with wake steering control.

It was also highlighted by Bossanyi (2019) how some turbines in the wind farm can benefit from preview information from the turbines situated further upstream. During 30 minute simulations, the slowly reacting yaw system was able to preemptively activate in anticipation of a change in direction. This effect was found to increase power production, while also reducing both the total yaw travel and the total number of yaw events significantly (yaw duty, Table 2).

850 An alternative method based on a simple GP regression method introduced in Section 6.3 was investigated by Van Der Hoek et al. (2021). It was found that unnecessary wind turbine yaw activity was reduced by $\approx 20\%$ through the use of an online version of the GP regression method incorporated into a collective yaw control system where the GP model was updated every 10-minutes with new measurements. However, the online model created less accurate predictions over time, indicating more sensitivity to the input data than the offline model and a need for greater refinement of the methodology.

855 7.3 Discussion of Wind Farm Flow Control

The performance of wind turbines clustered together in a farm is inextricably coupled with the farm flow conditions, especially the inflow wind direction. Therefore, wind farm flow control solutions that aim to regulate wind farm performance need to consider wind direction variability to be effective (Starke et al., 2021).

860 First of all, the use of robust control solutions that account for the uncertainties in input wind direction signals in their calculations have been shown to alleviate some of the problems associated with wind direction variability and bring about improvements in wake steering control (Rott et al., 2018; Quick et al., 2020) (Section 7.1). More understanding of the uncertainty bounds on control system inputs are needed in order to better evaluate the benefits and limitations of any given control approach (Shapiro et al., 2022).

865 Secondly, accurate wind direction measurement and estimation are critical for the implementation of successful wind farm and turbine controllers. Collective yaw control has been shown to offer slight improvements in power productions alongside substantial reductions in yaw activation (Bossanyi, 2019; Van Der Hoek et al., 2021) (Section 7.2). However, benefits were only seen in simple simulated scenarios over short time intervals, therefore more investigation is necessary.

8 Discussion

870 Wind farms are routinely subjected to changing wind directions, yet the effect on wind farms under realistic wind direction changes remains understudied (Shapiro et al., 2022). Accounting for the dynamic effect of these changes in high fidelity wind farm flow models has been shown to improve power output estimates (Munters et al., 2016) and result in more effective yaw and wake steering controllers compared to approaches that assume a static wind direction (Rott et al., 2018; Simley et al., 2020a).

875 Testing and validation of new control systems in simulations is essential before deployment in real world wind farms and relies on the use of wind farm flow models. These models need to make simplifying assumptions about the full flow field, and neglect most or at least some of the variability present in real-world conditions. These necessary assumptions have led to wind direction variability being mostly overlooked when it comes to assessing overall wind farm performance.

880 As discussed, most of the control-oriented modelling of wind direction up to the present has only been analysed over short time periods, in limited atmospheric conditions and with a focus purely on the objective of power gain and not overall performance improvements. Ultimately, research needs to assess the true impact of wind direction on wind farm performance, specifically the impact on LCOE. Hence, Section 8.1 introduces the critical challenges to be solved for this objective to be achieved.

8.1 Critical Challenges

885 From the literature, three critical technical challenges in control-oriented wind direction research can be identified. The three challenges are,

1. **Improved measurement of wind direction** - Reliable and comprehensive wind direction data needs to be obtained for model testing and validation along with agreement on standards of how wind direction should be measured and conditioned before use, particularly in relation to flow distortions, atmospheric stability and height above the surface. Measurement campaigns to produce large data sets for this specific purpose are imperative.
- 890 2. **Modelling realistic wind direction spatial and temporal variability with reasonable accuracy and computational cost** - Creation of validated and tested statistical and/or physical models that cover the full envelope of operational conditions are necessary to perform less computationally intensive data-driven wind farm flow simulations. Complementary to this, there is a parallel need for continued development of high fidelity meso-scale coupled LES models to analyse the important physical drivers of variability in more detail, as well as to better understand the interactions between wind
895 direction variability and wind turbine wakes.
3. **Development of a detailed scientific understanding of performance effects of wind direction variability and yaw misalignment on wind turbines and wind farms** - Extensive measurement campaigns are required to record turbine loads and power production data coupled with wind direction and yaw misalignment data. First and foremost, these measurements would allow for a proper scientific understanding of cause and effect. Only then can better control-oriented

900 models be designed and evaluated for prediction of power production and loads under yaw misalignment, which in turn can inform controller synthesis.

Addressing these challenges requires interdisciplinary research efforts that combine expertise from meteorology, control engineering, data science, and wind energy systems. Whilst the three critical challenges outlined above must be accomplished, there is a further critical dissemination challenge of embedding wind direction models within turbine and farm flow control
905 research, with respect to both design and testing. The first steps in this process are,

- Knowledge exchange and guidance for researchers in adjacent research areas as to the importance of wind direction modelling.
- Making wind direction models freely available and usable by researchers within other areas.

Tackling these challenges will have an important positive impact on wind turbine and farm modelling, design, and operational
910 analysis. It will contribute to improving performance and reliability, and ultimately help to reduce the LCOE of wind energy.

9 Conclusions

Wind direction variability plays a critical role in the operation and performance of wind farms. It is inherently non-linear and non-stationary due to complex atmospheric processes and the turbulent nature of wind flows. Additionally, wind direction varies both spatially and temporally, making it challenging to develop models that capture all of these effects at once. Site
915 specific conditions, such as wake and terrain effects, can also play a substantial role in wind farm performance.

The direction of the inflow relative to the rotor plane affects the aerodynamics of wind turbines in complex and unclear ways, which has implication for overall performance in terms of both power and loading. Incorporating such effects into wind farm flow models is important for controller design and testing. Wind farms are routinely subjected to changing wind directions, sometimes extreme changes, that need to be taken into account in wind farm flow control solutions that aim to regulate wind
920 farm performance (Starke et al., 2021). However, the uncertainty in wind direction measurements makes the assessment and implementation of control solutions more challenging, since accurate representations of cause and effect relationships for control purposes is difficult. The challenge is compounded by the fact that the behaviour of wind turbines and wind farm flow under realistic wind direction changes remains understudied (Shapiro et al., 2022).

The design of the yaw control system needs to incorporate important aspects of both physical analysis and statistical analysis,
925 such that it can optimise the turbine's operation while minimising the LCOE. The critical challenges associated with achieving this optimisation can be separated into three broad categories. These are; **improved measurements of wind direction, realistic dynamic wind direction modelling and farm and turbine performance effects of wind direction variability yaw misalignment.**

As wind energy plays an increasingly important role in global energy production, the development of accurate and versatile
930 control-oriented models will ensure the continued performance, reliability, efficiency and competitiveness of wind energy in the years to come.

Author contributions. Conceptualisation, S.D., A.S., and E.H.; writing—original draft preparation, S.D.; writing—review and editing, S.D., A.S. and E.H.; visualisation, S.D.; supervision, A.S., and E.H.; All authors have read and agreed to the published version of the manuscript.

Competing interests. The contact author has declared that none of the authors have any competing interests.

935 *Acknowledgements.* SD is funded by EP/S023801/1 EPSRC Centre for Doctoral Training in Wind and Marine Energy Systems and Structures, and would like to thank all of the staff involved in the CDT. EH is funded by a Brunel Fellowship from the Royal Commission for the Exhibition of 1851.

References

- Andrade, J. R. and Bessa, R. J.: Improving renewable energy forecasting with a grid of numerical weather predictions, *IEEE Transactions on Sustainable Energy*, 8, 1571–1580, <https://doi.org/10.1109/TSTE.2017.2694340>, 2017.
- 940 Annoni, J., Bay, C., Taylor, T., Pao, L., Fleming, P., and Johnson, K.: Efficient optimization of large wind farms for real-time control, in: 2018 Annual American Control Conference (ACC), pp. 6200–6205, IEEE, <https://doi.org/10.23919/ACC.2018.8430751>, 2018a.
- Annoni, J., Fleming, P., Scholbrock, A., Roadman, J., Dana, S., Adcock, C., Porte-Agel, F., Raach, S., Haizmann, F., and Schlipf, D.: Analysis of control-oriented wake modeling tools using lidar field results, *Wind Energy Science*, 3, 819–831, <https://doi.org/10.5194/wes-3-819-2018>, 2018b.
- 945 Annoni, J., Bay, C., Johnson, K., Dall’Anese, E., Quon, E., Kemper, T., and Fleming, P.: Wind direction estimation using SCADA data with consensus-based optimization, *Wind Energy Science*, 4, 355–368, <https://doi.org/10.5194/wes-4-355-2019>, 2019a.
- Annoni, J., Dall’Anese, E., Hong, M., and Bay, C. J.: Efficient distributed optimization of wind farms using proximal primal-dual algorithms, in: 2019 American Control Conference (ACC), pp. 4173–4178, IEEE, <https://doi.org/10.23919/ACC.2019.8814655>, 2019b.
- 950 Bao, L., Gneiting, T., Gritmit, E. P., Guttorp, P., and Raftery, A. E.: Bias correction and Bayesian model averaging for ensemble forecasts of surface wind direction, *Monthly Weather Review*, 138, 1811–1821, <https://doi.org/10.1175/2009MWR3138.1>, 2010.
- Barthelmie, R. J., Wang, H., Doubrawa, P., and Pryor, S.: Best practice for measuring wind speeds and turbulence offshore through in-situ and remote sensing technologies, <https://doi.org/10.7298/X4QV3JGF>, 2016.
- Bartl, J., Mühle, F., and Sætran, L.: Wind tunnel study on power output and yaw moments for two yaw-controlled model wind turbines, *Wind Energy Science*, 3, 489–502, <https://doi.org/10.5194/wes-3-489-2018>, 2018.
- 955 Bay, C. J., Annoni, J., Taylor, T., Pao, L., and Johnson, K.: Active power control for wind farms using distributed model predictive control and nearest neighbor communication, in: 2018 Annual American Control Conference (ACC), pp. 682–687, IEEE, <https://doi.org/10.23919/ACC.2018.8431764>, 2018.
- Bernardoni, F., Ciri, U., Rotea, M., and Leonardi, S.: Real-time identification of clusters of turbines, in: *Journal of Physics: Conference Series*, vol. 1618, p. 022032, IOP Publishing, <https://doi.org/10.1088/1742-6596/1618/2/022032>, 2020.
- 960 Bernardoni, F., Ciri, U., Rotea, M. A., and Leonardi, S.: Identification of turbine clusters during time varying wind direction, in: 2022 American Control Conference (ACC), pp. 4236–4241, IEEE, <https://doi.org/10.23919/ACC53348.2022.9867223>, 2022.
- Bivona, S., Bonanno, G., Burlon, R., Gurrera, D., and Leone, C.: Stochastic models for wind speed forecasting, *Energy conversion and management*, 52, 1157–1165, <https://doi.org/10.1016/j.enconman.2010.09.010>, 2011.
- 965 Boersma, S.: Towards closed-loop dynamical wind farm control: model development and control applications, Ph.D. thesis, Delft University of Technology, <https://doi.org/10.4233/uuid:48572080-bc51-4ffe-9ba5-676ee9ab5fcc>, 2019.
- Boersma, S., Doekemeijer, B. M., Gebraad, P. M., Fleming, P. A., Annoni, J., Scholbrock, A. K., Frederik, J. A., and van Wingerden, J.-W.: A tutorial on control-oriented modeling and control of wind farms, in: 2017 American control conference (ACC), pp. 1–18, IEEE, <http://doi.org/10.23919/ACC.2017.7962923>, 2017.
- 970 Bossanyi, E.: Combining induction control and wake steering for wind farm energy and fatigue loads optimisation, vol. 1037, p. 032011, IOP Publishing, <https://doi.org/10.1088/1742-6596/1037/3/032011>, 2018.
- Bossanyi, E.: Optimising yaw control at wind farm level, *Journal of Physics: Conference Series*, 1222, <https://doi.org/10.1088/1742-6596/1222/1/012023>, 2019.

- Bossanyi, E. and Ruisi, R.: Axial induction controller field test at Sedini wind farm, *Wind Energy Science*, 6, 389–408, <https://doi.org/10.5194/wes-6-389-2021>, 2021.
- 975
- Breedt, H. J., Craig, K. J., and Jothiprakasam, V. D.: Monin-Obukhov similarity theory and its application to wind flow modelling over complex terrain, *Journal of Wind Engineering and Industrial Aerodynamics*, 182, 308–321, <https://doi.org/10.1016/j.jweia.2018.09.026>, 2018.
- Calaf, M., Meneveau, C., and Meyers, J.: Large eddy simulation study of fully developed wind-turbine array boundary layers, *Physics of fluids*, 22, 015 110, <https://doi.org/10.1063/1.3291077>, 2010.
- 980
- Campagnolo, F., Weber, R., Schreiber, J., and Bottasso, C. L.: Wind tunnel testing of wake steering with dynamic wind direction changes, *Wind Energy Science*, 5, 1273–1295, <https://doi.org/10.5194/wes-5-1273-2020>, 2020.
- Cardaun, M., Roscher, B., Schelenz, R., and Jacobs, G.: Analysis of wind-turbine main bearing loads due to constant yaw misalignments over a 20 years timespan, *Energies*, 12, 1768, <https://doi.org/10.3390/en12091768>, 2019.
- 985
- Carvalho, D., Rocha, A., Gómez-Gesteira, M., and Santos, C.: A sensitivity study of the WRF model in wind simulation for an area of high wind energy, *Environmental Modelling & Software*, 33, 23–34, 2012.
- Chan, P. and Hon, K.: Performance of super high resolution numerical weather prediction model in forecasting terrain-disrupted airflow at the Hong Kong International Airport: case studies, *Meteorological Applications*, 23, 101–114, <https://doi.org/10.1002/met.1534>, 2016.
- Chatterjee, T., Cherukuru, N. W., Peet, Y. T., and Calhoun, R. J.: Large eddy simulation with realistic geophysical inflow of Alpha Ventus
- 990
- wind farm: a comparison with LIDAR field experiments, in: *Journal of Physics: Conference Series*, vol. 1037, p. 072056, IOP Publishing, <https://doi.org/10.1088/1742-6596/1037/7/072056>, 2018.
- Chen, W., Liu, H., Lin, Y., Li, W., Sun, Y., and Zhang, D.: LSTM-NN yaw control of wind turbines based on upstream wind information, *Energies*, 13, 1482, <https://doi.org/10.3390/en13061482>, 2020.
- Chen, W., Qian, G., Qi, W., Luo, G., Zhao, L., and Yuan, X.: Layout Method of Met Mast Based on Macro Zoning and Micro Quantitative
- 995
- Siting in a Wind Farm, *Processes*, 10, 1708, <https://doi.org/10.3390/pr10091708>, 2022.
- Chitsazan, M. A., Fadali, M. S., and Trzynadlowski, A. M.: Wind speed and wind direction forecasting using echo state network with nonlinear functions, *Renewable energy*, 131, 879–889, <https://doi.org/10.1016/j.renene.2018.07.060>, 2019.
- Coleman, J. and Law, K.: *Meteorology*, Elsevier, <https://doi.org/10.1016/B978-0-12-409548-9.09492-6>, 2015.
- Cortina, G., Sharma, V., and Calaf, M.: Investigation of the incoming wind vector for improved wind turbine yaw-adjustment under different
- 1000
- atmospheric and wind farm conditions, *Renewable Energy*, 101, 376–386, <https://doi.org/10.1016/j.renene.2016.08.011>, 2017.
- Cremers, J. and Klugkist, I.: One direction? A tutorial for circular data analysis using R with examples in cognitive psychology, *Frontiers in psychology*, 9, 2040, <https://doi.org/10.3389/fpsyg.2018.02040>, 2018.
- Damiani, R., Dana, S., Annoni, J., Fleming, P., Roadman, J., van Dam, J., and Dykes, K.: Assessment of wind turbine component loads under yaw-offset conditions, *Wind Energy Science*, 3, 173–189, <https://doi.org/10.5194/wes-3-173-2018>, 2018.
- 1005
- Davies, B. M. and Thomson, D. J.: Comparisons of some parametrizations of wind direction variability with observations, *Atmospheric Environment*, 33, 4909–4917, [https://doi.org/10.1016/S1352-2310\(99\)00287-3](https://doi.org/10.1016/S1352-2310(99)00287-3), 1999.
- Doekemeijer, B. M., Boersma, S., Pao, L. Y., Knudsen, T., and van Wingerden, J.-W.: Online model calibration for a simplified LES model in pursuit of real-time closed-loop wind farm control, *Wind Energy Science*, 3, 749–765, <https://doi.org/10.5194/wes-3-749-2018>, 2018.
- Dong, L., Lio, W. H., and Simley, E.: On turbulence models and lidar measurements for wind turbine control, *Wind Energy Science*, 6,
- 1010
- 1491–1500, <https://doi.org/10.5194/wes-6-1491-2021>, 2021.

- Draper, M., Guggeri, A., López, B., Díaz, A., Campagnolo, F., and Usera, G.: A Large Eddy Simulation framework to assess wind farm power maximization strategies: Validation of maximization by yawing, in: *Journal of Physics: Conference Series*, vol. 1037, p. 072051, IOP Publishing, <https://doi.org/10.1088/1742-6596/1037/7/072051>, 2018.
- 1015 Draxl, C.: On the predictability of hub height winds, <https://orbit.dtu.dk/en/publications/on-the-predictability-of-hub-height-winds> Accessed: 22.08.2022, 2012.
- Draxl, C., Allaerts, D., Quon, E., and Churchfield, M.: Coupling mesoscale budget components to large-eddy simulations for wind-energy applications, *Boundary-Layer Meteorology*, 179, 73–98, <https://doi.org/10.1007/s10546-020-00584-z>, 2021.
- Eecen, P., Wagenaar, J., Stefanatos, N., Pedersen, T. F., Wagner, R., and Hansen, K. S.: UPWIND 1A2 Metrology. Final Report, <https://orbit.dtu.dk/en/publications/upwind-1a2-metrology-final-report> Accessed: 26.08.2022, 2011.
- 1020 El-Fouly, T. H., El-Saadany, E. F., and Salama, M. M.: One day ahead prediction of wind speed and direction, *IEEE transactions on energy conversion*, 23, 191–201, <https://doi.org/10.1109/TEC.2007.905069>, 2008.
- Energy, S. G. R.: Onshore product portfolio, Brochure, <https://www.siemensgamesa.com/en-int/-/media/siemensgamesa/downloads/en-products-and-services/onshore/brochures/siemens-gamesa-onshore-product-portfolio-en.pdf> Accessed: 16.09.2022, 2022.
- Erdem, E. and Shi, J.: ARMA based approaches for forecasting the tuple of wind speed and direction, *Applied Energy*, 88, 1405–1414, <https://doi.org/10.1016/j.apenergy.2010.10.031>, 2011.
- 1025 Etling, D.: On plume meandering under stable stratification, *Atmospheric Environment. Part A. General Topics*, 24, 1979–1985, [https://doi.org/10.1016/0960-1686\(90\)90232-C](https://doi.org/10.1016/0960-1686(90)90232-C), 1990.
- Farret, F. A., Pfitscher, L. L., and Bernardon, D. P.: Sensorless active yaw control for wind turbines, in: *IECON'01. 27th Annual Conference of the IEEE Industrial Electronics Society (Cat. No. 37243)*, vol. 2, pp. 1370–1375, IEEE, <https://doi.org/10.1109/IECON.2001.975981>, 2001.
- 1030 Farrugia, P. S. and Micallef, A.: Vectorial statistics for the standard deviation of wind direction, *Meteorology and Atmospheric Physics*, 129, 495–506, <https://doi.org/10.1007/s00703-016-0483-8>, 2017.
- Farrugia, P. S., Borg, J. L., and Micallef, A.: On the algorithms used to compute the standard deviation of wind direction, *Journal of Applied Meteorology and Climatology*, 48, 2144–2151, <https://doi.org/10.1175/2009JAMC2050.1>, 2009.
- 1035 Feijóo, A. and Villanueva, D.: Contributions to wind farm power estimation considering wind direction-dependent wake effects, *Wind Energy*, 20, 221–231, <https://doi.org/10.1002/we.2002>, 2017.
- Fisher, N. and Lee, A.: Time series analysis of circular data, *Journal of the Royal Statistical Society: Series B (Methodological)*, 56, 327–339, <https://doi.org/10.1111/j.2517-6161.1994.tb01981.x>, 1994.
- Fisher, N. I.: *Statistical analysis of circular data*, cambridge university press, 1995.
- 1040 Fleming, P., Gebraad, P. M., Lee, S., van Wingerden, J.-W., Johnson, K., Churchfield, M., Michalakes, J., Spalart, P., and Moriarty, P.: Simulation comparison of wake mitigation control strategies for a two-turbine case, *Wind Energy*, 18, 2135–2143, <https://doi.org/10.1002/we.1810>, 2015.
- Fleming, P., Churchfield, M., Scholbrock, A., Clifton, A., Schreck, S., Johnson, K., Wright, A., Gebraad, P., Annoni, J., Naughton, B., et al.: Detailed field test of yaw-based wake steering, in: *Journal of Physics: Conference Series*, vol. 753, p. 052003, IOP Publishing, <https://dx.doi.org/10.1088/1742-6596/753/5/052003>, 2016.
- 1045 Fleming, P., Annoni, J., Shah, J. J., Wang, L., Ananthan, S., Zhang, Z., Hutchings, K., Wang, P., Chen, W., and Chen, L.: Field test of wake steering at an offshore wind farm, *Wind Energy Science*, 2, 229–239, <https://doi.org/10.5194/wes-2-229-2017>, 2017.

- Fleming, P., King, J., Dykes, K., Simley, E., Roadman, J., Scholbrock, A., Murphy, P., Lundquist, J. K., Moriarty, P., Fleming, K., et al.: Initial results from a field campaign of wake steering applied at a commercial wind farm—Part 1, *Wind Energy Science*, 4, 273–285, <https://doi.org/10.5194/wes-4-273-2019>, 2019.
- 1050 Fleming, P. A., Gebraad, P. M., Lee, S., van Wingerden, J.-W., Johnson, K., Churchfield, M., Michalakes, J., Spalart, P., and Moriarty, P.: Evaluating techniques for redirecting turbine wakes using SOWFA, *Renewable Energy*, 70, 211–218, <https://doi.org/10.1016/j.renene.2014.02.015>, 2014a.
- Fleming, P. A., Scholbrock, A., Jehu, A., Davoust, S., Osler, E., Wright, A. D., and Clifton, A.: Field-test results using a nacelle-mounted lidar for improving wind turbine power capture by reducing yaw misalignment, in: *Journal of Physics: Conference Series*, vol. 524, p. 012002, IOP Publishing, <https://doi.org/10.1088/1742-6596/524/1/012002>, 2014b.
- 1055 Gaumond, M., Réthoré, P.-E., Bechmann, A., Ott, S., Larsen, G. C., Peña, A., and Hansen, K. S.: Benchmarking of wind turbine wake models in large offshore wind farms, in: *Proceedings of the science of making torque from wind conference*, 2012.
- Gaumond, M., Réthoré, P.-E., Ott, S., Pena, A., Bechmann, A., and Hansen, K. S.: Evaluation of the wind direction uncertainty and its impact on modeling at the Horns Rev offshore wind farm, *Wind Energy*, 17, 1169–1178, <https://doi.org/10.1002/we.1625>, 2014.
- 1060 Gebraad, P. M., Teeuwisse, F., van Wingerden, J.-W., Fleming, P. A., Ruben, S. D., Marden, J. R., and Pao, L. Y.: A data-driven model for wind plant power optimization by yaw control, in: *2014 American Control Conference*, pp. 3128–3134, IEEE, <https://doi.org/10.1109/ACC.2014.6859118>, 2014.
- Gebraad, P. M., Teeuwisse, F., Van Wingerden, J., Fleming, P. A., Ruben, S., Marden, J., and Pao, L.: Wind plant power optimization through yaw control using a parametric model for wake effects—a CFD simulation study, *Wind Energy*, 19, 95–114, <https://doi.org/10.1002/we.1822>, 2016.
- 1065 Goit, J. P., Munters, W., and Meyers, J.: Optimal coordinated control of power extraction in LES of a wind farm with entrance effects, *Energies*, 9, 29, <https://doi.org/10.3390/en9010029>, 2016.
- Hanna, S.: Lateral dispersion in light-wind stable conditions, *Il Nuovo Cimento C*, 13, 889–894, <https://doi.org/10.1007/BF02514777>, 1990.
- 1070 Hanna, S. R.: Lateral turbulence intensity and plume meandering during stable conditions, *Journal of Applied Meteorology and Climatology*, 22, 1424–1430, [https://doi.org/10.1175/1520-0450\(1983\)022%3C1424:LTIAPM%3E2.0.CO;2](https://doi.org/10.1175/1520-0450(1983)022%3C1424:LTIAPM%3E2.0.CO;2), 1983.
- Hans, A. P. and Jhon, A.: *Atmospheric turbulence, models and methods for engineering applications*, Wiley, New York, 1984.
- Hart, E., Stock, A., Elderfield, G., Elliott, R., Brasseur, J., Keller, J., Guo, Y., and Song, W.: Impacts of wind field characteristics and non-steady deterministic wind events on time-varying main-bearing loads, *Wind Energy Science*, 7, 1209–1226, <https://doi.org/10.5194/wes-7-1209-2022>, 2022.
- 1075 Hau, E.: *Wind turbines: fundamentals, technologies, application, economics*, Springer Science & Business Media, <https://doi.org/10.1007/978-3-642-27151-9>, 2013.
- Haupt, S., Anderson, A., Berg, L., Brown, B., Churchfield, M., Draxl, C., Ennis, B., Feng, Y., Kosovic, B., Kotamarthi, R., et al.: First year report of the a2e mesoscale to microscale coupling project, Pacific Northwest National Laboratory, Tech. Report PNNL-25108, 2015.
- 1080 Haupt, S., Berg, L., Churchfield, M., Kosovic, B., Mirocha, J., and Shaw, W.: Mesoscale to microscale coupling for wind energy applications: Addressing the challenges, in: *Journal of Physics: Conference Series*, vol. 1452, p. 012076, IOP Publishing, <https://doi.org/10.1088/1742-6596/1452/1/012076>, 2020.
- Haupt, S. E., Kotamarthi, R., Feng, Y., Mirocha, J. D., Koo, E., Linn, R., Kosovic, B., Brown, B., Anderson, A., Churchfield, M. J., et al.: Second year report of the atmosphere to electrons mesoscale to microscale coupling project: Nonstationary modeling techniques and

- 1085 assessment, Tech. rep., Pacific Northwest National Lab.(PNNL), Richland, WA (United States), <https://www.osti.gov/biblio/1573811> Accessed: 01.09.2022, 2017.
- Haupt, S. E., Kosovic, B., Shaw, W., Berg, L. K., Churchfield, M., Cline, J., Draxl, C., Ennis, B., Koo, E., Kotamarthi, R., et al.: On bridging a modeling scale gap: Mesoscale to microscale coupling for wind energy, *Bulletin of the American Meteorological Society*, 100, 2533–2550, <https://doi.org/10.1175/BAMS-D-18-0033.1>, 2019.
- 1090 Heck, K. S., Johlas, H. M., and Howland, M. F.: Modelling the induction, thrust and power of a yaw-misaligned actuator disk, *Journal of Fluid Mechanics*, 959, A9, <https://doi.org/10.1017/jfm.2023.129>, 2023.
- Hirata, Y., Mandic, D. P., Suzuki, H., and Aihara, K.: Wind direction modelling using multiple observation points, *Philosophical Transactions of the Royal Society A: Mathematical, Physical and Engineering Sciences*, 366, 591–607, <https://doi.org/10.1098/rsta.2007.2112>, 2008.
- Houck, D. R.: Review of wake management techniques for wind turbines, *Wind Energy*, 25, 195–220, <https://doi.org/10.1002/we.2668>, 2022.
- 1095 Howland, M. F.: Wind farm yaw control set-point optimization under model parameter uncertainty, *Journal of Renewable and Sustainable Energy*, 13, 043 303, <https://doi.org/10.1063/5.0051071>, 2021.
- Howland, M. F., Lele, S. K., and Dabiri, J. O.: Wind farm power optimization through wake steering, *Proceedings of the National Academy of Sciences*, 116, 14 495–14 500, <https://doi.org/10.1073/pnas.1903680116>, 2019.
- Howland, M. F., González, C. M., Martínez, J. J. P., Quesada, J. B., Larranaga, F. P., Yadav, N. K., Chawla, J. S., and Dabiri, J. O.: Influence of atmospheric conditions on the power production of utility-scale wind turbines in yaw misalignment, *Journal of Renewable and Sustainable Energy*, 12, 063 307, <https://doi.org/10.1063/5.0023746>, 2020.
- Howland, M. F., Ghate, A. S., Quesada, J. B., Pena Martínez, J. J., Zhong, W., Larrañaga, F. P., Lele, S. K., and Dabiri, J. O.: Optimal closed-loop wake steering–Part 2: Diurnal cycle atmospheric boundary layer conditions, *Wind Energy Science*, 7, 345–365, <https://doi.org/10.5194/wes-7-345-2022>, 2022a.
- 1105 Howland, M. F., Quesada, J. B., Martínez, J. J. P., Larrañaga, F. P., Yadav, N., Chawla, J. S., Sivaram, V., and Dabiri, J. O.: Collective wind farm operation based on a predictive model increases utility-scale energy production, *Nature Energy*, 7, 818–827, <https://doi.org/10.1038/s41560-022-01085-8>, 2022b.
- Jammalamadaka, S. R. and SenGupta, A.: *Topics in circular statistics*, vol. 5, world scientific, <https://doi.org/10.1142/4031>, 2001.
- Jiménez, P. A. and Dudhia, J.: On the ability of the WRF model to reproduce the surface wind direction over complex terrain, *Journal of Applied Meteorology and Climatology*, 52, 1610–1617, <https://doi.org/10.1175/JAMC-D-12-0266.1>, 2013.
- 1110 Joffre, S. M. and Laurila, T.: Standard deviations of wind speed and direction from observations over a smooth surface, *Journal of Applied Meteorology and Climatology*, 27, 550–561, [https://doi.org/10.1175/1520-0450\(1988\)027%3C0550:SDOWSA%3E2.0.CO;2](https://doi.org/10.1175/1520-0450(1988)027%3C0550:SDOWSA%3E2.0.CO;2), 1988.
- Karakasis, N., Mesemanolis, A., Nalmpantis, T., and Mademlis, C.: Active yaw control in a horizontal axis wind system without requiring wind direction measurement, *IET Renewable Power Generation*, 10, 1441–1449, <https://doi.org/10.1049/iet-rpg.2016.0005>, 2016.
- 1115 Karami, F., Zhang, Y., Rotea, M. A., Bernardoni, F., and Leonardi, S.: Real-time Wind Direction Estimation using Machine Learning on Operational Wind Farm Data, in: 2021 60th IEEE Conference on Decision and Control (CDC), pp. 2456–2461, IEEE, <https://doi.org/10.23919/ACC53348.2022.9867223>, 2021.
- Kau, W., Lee, H., and Kao, S.: A statistical model for wind prediction at a mountain and valley station near Anderson Creek, California, *Journal of Applied Meteorology (1962-1982)*, pp. 18–21, <https://www.jstor.org/stable/26180207>, 1982.
- 1120 Kheirabadi, A. C. and Nagamune, R.: A quantitative review of wind farm control with the objective of wind farm power maximization, *Journal of Wind Engineering and Industrial Aerodynamics*, 192, 45–73, <https://doi.org/10.1016/j.jweia.2019.06.015>, 2019.

- Kheirabadi, A. C. and Nagamune, R.: A low-fidelity dynamic wind farm model for simulating time-varying wind conditions and floating platform motion, *Ocean Engineering*, 234, 109 313, <https://doi.org/10.1016/j.oceaneng.2021.109313>, 2021.
- Kim, J. H.: Forecasting autoregressive time series with bias-corrected parameter estimators, *International Journal of Forecasting*, 19, 493–502, 2003.
- Kim, M. and Dalhoff, P.: Yaw Systems for wind turbines—Overview of concepts, current challenges and design methods, in: *Journal of Physics: Conference Series*, vol. 524, p. 012086, IOP Publishing, <https://doi.org/10.1088/1742-6596/524/1/012086>, 2014.
- Kooijman, H., Lindenburg, C., Winkelaar, D., and Van der Hooft, E.: DOWEC 6 MW Pre-Design: Aero-elastic modeling of the DOWEC 6 MW pre-design in PHATAS, DOWEC Dutch Offshore Wind Energy Converter 1997–2003 Public Reports, 2003.
- 1130 Kragh, K. and Fleming, P.: Rotor speed dependent yaw control of wind turbines based on empirical data, in: 50th AIAA Aerospace Sciences Meeting including the New Horizons Forum and Aerospace Exposition, p. 1018, <https://doi.org/10.2514/6.2012-1018>, 2012.
- Kragh, K., Hansen, M., and Mikkelsen, T.: Improving yaw alignment using spinner based LIDAR, in: 49th AIAA Aerospace Sciences Meeting including the New Horizons Forum and Aerospace Exposition, p. 264, <https://doi.org/10.2514/6.2011-264>, 2011.
- Kragh, K. A. and Hansen, M. H.: Load alleviation of wind turbines by yaw misalignment, *Wind Energy*, 17, 971–982, <https://doi.org/10.1002/we.1612>, 2014.
- 1135 Kragh, K. A. and Hansen, M. H.: Potential of power gain with improved yaw alignment, *Wind Energy*, 18, 979–989, <https://doi.org/10.1002/we.1739>, 2015.
- Kragh, K. A., Fleming, P. A., and Scholbrock, A. K.: Increased power capture by rotor speed-dependent yaw control of wind turbines, *Journal of solar energy engineering*, 135, <https://doi.org/10.1115/1.4023971>, 2013a.
- 1140 Kragh, K. A., Hansen, M. H., and Mikkelsen, T.: Precision and shortcomings of yaw error estimation using spinner-based light detection and ranging, *Wind Energy*, 16, 353–366, <https://doi.org/10.1002/we.1492>, 2013b.
- Kristensen, L., Jensen, N. O., and Petersen, E. L.: Lateral dispersion of pollutants in a very stable atmosphere—the effect of meandering, *Atmospheric Environment (1967)*, 15, 837–844, [https://doi.org/10.1016/0004-6981\(81\)90288-2](https://doi.org/10.1016/0004-6981(81)90288-2), 1981.
- Krogstad, P.-Å. and Adaramola, M. S.: Performance and near wake measurements of a model horizontal axis wind turbine, *Wind Energy*, 15, 743–756, <https://doi.org/10.1002/we.502>, 2012.
- 1145 Larsen, G. C., Larsen, T. J., and Chougule, A.: Medium fidelity modelling of loads in wind farms under non-neutral ABL stability conditions—a full-scale validation study, in: *Journal of Physics: Conference Series*, vol. 854, p. 012026, IOP Publishing, <https://doi.org/10.1088/1742-6596/854/1/012026>, 2017.
- Li, J.-Q. J., Yang, X. I., and Kunz, R. F.: Grid-point and time-step requirements for large-eddy simulation and Reynolds-averaged Navier–Stokes of stratified wakes, *Physics of Fluids*, 34, 115 125, <https://doi.org/10.1063/5.0127487>, 2022.
- 1150 Mahrt, L.: Mesoscale wind direction shifts in the stable boundary-layer, *Tellus A: Dynamic Meteorology and Oceanography*, 60, 700–705, <https://doi.org/10.1111/j.1600-0870.2007.00324.x>, 2008.
- Mahrt, L.: Surface wind direction variability, *Journal of applied meteorology and climatology*, 50, 144–152, <https://doi.org/10.1175/2010JAMC2560.1>, 2011.
- 1155 Mann, J.: Wind field simulation, *Probabilistic engineering mechanics*, 13, 269–282, [https://doi.org/10.1016/S0266-8920\(97\)00036-2](https://doi.org/10.1016/S0266-8920(97)00036-2), 1998.
- Mardia, K. V., Jupp, P. E., and Mardia, K.: *Directional statistics*, vol. 2, Wiley Online Library, 2000.
- Medici, D.: Experimental studies of wind turbine wakes: power optimisation and meandering, Ph.D. thesis, KTH, <http://kth.diva-portal.org/smash/record.jsf?pid=diva2%3A14563&dsid=5900> Accessed:09/03/22, 2005.

- Meyers, J., Bottasso, C., Dykes, K., Fleming, P., Gebraad, P., Giebel, G., Göçmen, T., and van Wingerden, J.-W.: Wind farm flow control: prospects and challenges, *Wind Energy Science Discussions*, pp. 1–56, <https://doi.org/10.5194/wes-2022-24>, 2022.
- 1160 Mikkelsen, T., Hansen, K. H., Angelou, N., Sjöholm, M., Harris, M., Hadley, P., Scullion, R., Ellis, G., and Vives, G.: Lidar wind speed measurements from a rotating spinner, in: *European Wind Energy Conference and Exhibition*, https://backend.orbit.dtu.dk/ws/portalfiles/portal/4553836/Mikkelsen_EWEC_2010.pdf Accessed: 23.08.2022, 2010.
- Mikkelsen, T., Angelou, N., Hansen, K., Sjöholm, M., Harris, M., Slinger, C., Hadley, P., Scullion, R., Ellis, G., and Vives, G.: A spinner-integrated wind lidar for enhanced wind turbine control, *Wind Energy*, 16, 625–643, <https://doi.org/10.1002/we.1564>, 2013.
- 1165 Mirocha, J., Kosović, B., and Kirkil, G.: Resolved turbulence characteristics in large-eddy simulations nested within mesoscale simulations using the Weather Research and Forecasting Model, *Monthly Weather Review*, 142, 806–831, <https://doi.org/10.1175/MWR-D-13-00064.1>, 2014.
- Muñoz-Esparza, D. and Kosović, B.: Generation of inflow turbulence in large-eddy simulations of nonneutral atmospheric boundary layers with the cell perturbation method, *Monthly Weather Review*, 146, 1889–1909, <https://doi.org/10.1175/MWR-D-18-0077.1>, 2018.
- 1170 Muñoz-Esparza, D., Kosović, B., Mirocha, J., and van Beeck, J.: Bridging the transition from mesoscale to microscale turbulence in numerical weather prediction models, *Boundary-layer meteorology*, 153, 409–440, <https://doi.org/10.1007/s10546-014-9956-9>, 2014.
- Munters, W., Meneveau, C., and Meyers, J.: Turbulent inflow precursor method with time-varying direction for large-eddy simulations and applications to wind farms, *Boundary-layer meteorology*, 159, 305–328, <https://doi.org/10.1007/s10546-016-0127-z>, 2016.
- 1175 Ouyang, T., Kusiak, A., and He, Y.: Predictive model of yaw error in a wind turbine, *Energy*, 123, 119–130, <https://doi.org/10.1016/j.energy.2017.01.150>, 2017.
- Pao, L. Y. and Johnson, K. E.: A tutorial on the dynamics and control of wind turbines and wind farms, in: *2009 American Control Conference*, pp. 2076–2089, IEEE, <https://doi.org/10.1109/ACC.2009.5160195>, 2009.
- Pedersen, T., Vita, L., Sørensen, N., and Enevoldsen, P.: Operational experiences with a spinner anemometer on a MW size wind turbine, *EWEC2008*, Bruxelles, <https://www.osti.gov/etdweb/servlets/purl/946864> Accessed: 17.08.2022, 2008.
- 1180 Pedersen, T. F., Gottschall, J., Kristoffersen, J. R., and Dahlberg, J.-Å.: Yawing and performance of an offshore wind farm, in: *EWEA Annual Event 2011*, European Wind Energy Association (EWEA), <https://orbit.dtu.dk/en/publications/yawing-and-performance-of-an-offshore-wind-farm> Accessed: 23.08.2022, 2011.
- Peña, A. and Hahmann, A. N.: Atmospheric stability and turbulence fluxes at Horns Rev—An intercomparison of sonic, bulk and WRF model data, *Wind Energy*, 15, 717–731, <https://doi.org/10.1002/we.500>, 2012.
- 1185 Porté-Agel, F., Wu, Y.-T., and Chen, C.-H.: A numerical study of the effects of wind direction on turbine wakes and power losses in a large wind farm, *Energies*, 6, 5297–5313, <https://doi.org/10.3390/en6105297>, 2013.
- Porté-Agel, F., Bastankhah, M., and Shamsoddin, S.: Wind-turbine and wind-farm flows: a review, *Boundary-Layer Meteorology*, 174, 1–59, <https://doi.org/10.1007/s10546-019-00473-0>, 2020.
- 1190 Quick, J., Annoni, J., King, R., Dykes, K., Fleming, P., and Ning, A.: Optimization under uncertainty for wake steering strategies, in: *Journal of physics: Conference series*, vol. 854, p. 012036, IOP Publishing, <https://doi.org/10.1088/1742-6596/854/1/012036>, 2017.
- Quick, J., King, J., King, R. N., Hamlington, P. E., and Dykes, K.: Wake steering optimization under uncertainty, *Wind Energy Science*, 5, 413–426, <https://doi.org/10.5194/wes-5-413-2020>, 2020.
- Rasmussen, C. E.: Gaussian processes in machine learning, in: *Summer school on machine learning*, pp. 63–71, Springer, https://doi.org/10.1007/978-3-540-28650-9_4, 2003.
- 1195

- Rott, A., Doekemeijer, B., Seifert, J. K., van Wingerden, J.-W., and Kühn, M.: Robust active wake control in consideration of wind direction variability and uncertainty, *Wind energy science*, 3, 869–882, <https://doi.org/10.5194/wes-3-869-2018>, 2018.
- Sanz Rodrigo, J., Chávez Arroyo, R. A., Moriarty, P., Churchfield, M., Kosović, B., Réthoré, P.-E., Hansen, K. S., Hahmann, A., Mirocha, J. D., and Rife, D.: Mesoscale to microscale wind farm flow modeling and evaluation, *Wiley Interdisciplinary Reviews: Energy and Environment*, 6, e214, <https://doi.org/10.1002/wene.214>, 2017.
- Schalkwijk, J., Jonker, H. J., Siebesma, A. P., and Bosveld, F. C.: A year-long large-eddy simulation of the weather over Cabauw: An overview, *Monthly Weather Review*, 143, 828–844, <https://doi.org/10.1175/MWR-D-14-00293.1>, 2015.
- Schepers, J., Boorsma, K., and Munduate, X.: Final Results from Mexnext-I: Analysis of detailed aerodynamic measurements on a 4.5 m diameter rotor placed in the large German Dutch Wind Tunnel DNW, in: *Journal of Physics: Conference Series*, vol. 555, p. 012089, IOP Publishing, <https://doi.org/10.1088/1742-6596/555/1/012089>, 2014.
- Scholbrock, A., Fleming, P., Schlipf, D., Wright, A., Johnson, K., and Wang, N.: Lidar-enhanced wind turbine control: Past, present, and future, in: *2016 American Control Conference (ACC)*, pp. 1399–1406, IEEE, <https://doi.org/10.1109/ACC.2016.7525113>, 2016.
- Schreiber, J., Nanos, E., Campagnolo, F., and Bottasso, C. L.: Verification and calibration of a reduced order wind farm model by wind tunnel experiments, in: *Journal of Physics: Conference Series*, vol. 854, p. 012041, IOP Publishing, <https://doi.org/10.1088/1742-6596/854/1/012041>, 2017.
- Schreiber, J., Bottasso, C. L., Salbert, B., and Campagnolo, F.: Improving wind farm flow models by learning from operational data, *Wind Energy Science*, 5, 647–673, <https://doi.org/10.5194/wes-5-647-2020>, 2020.
- Shapiro, C. R., Starke, G. M., Meneveau, C., and Gayme, D. F.: A wake modeling paradigm for wind farm design and control, *Energies*, 12, 2956, <https://doi.org/10.3390/en12152956>, 2019.
- Shapiro, C. R., Starke, G. M., and Gayme, D. F.: Turbulence and control of wind farms, *Annual Review of Control, Robotics, and Autonomous Systems*, 5, 579–602, <https://doi.org/10.1146/annurev-control-070221-114032>, 2022.
- Simley, E., Pao, L. Y., Frehlich, R., Jonkman, B., and Kelley, N.: Analysis of light detection and ranging wind speed measurements for wind turbine control, *Wind Energy*, 17, 413–433, <https://doi.org/10.1002/we.1584>, 2014.
- Simley, E., Fleming, P., and King, J.: Design and analysis of a wake steering controller with wind direction variability, *Wind Energy Science*, 5, 451–468, <https://doi.org/10.5194/wes-5-451-2020>, 2020a.
- Simley, E., Fleming, P., and King, J.: Field validation of wake steering control with wind direction variability, in: *Journal of Physics: Conference Series*, vol. 1452, p. 012012, IOP Publishing, <https://doi.org/10.1088/1742-6596/1452/1/012012>, 2020b.
- Simley, E., Fleming, P., King, J., and Sinner, M.: Wake steering wind farm control with preview wind direction information, Tech. rep., National Renewable Energy Lab.(NREL), Golden, CO (United States), 2021.
- Sinner, M., Pao, L. Y., and King, J.: Estimation of large-scale wind field characteristics using supervisory control and data acquisition measurements, in: *2020 American Control Conference (ACC)*, pp. 2357–2362, IEEE, <https://doi.org/10.23919/ACC45564.2020.9147859>, 2020.
- Sinner, M., Simley, E., King, J., Fleming, P., and Pao, L. Y.: Power increases using wind direction spatial filtering for wind farm control: Evaluation using FLORIS, modified for dynamic settings, *Journal of Renewable and Sustainable Energy*, 13, 023 310, <https://doi.org/10.1063/5.0039899>, 2021.
- Smith, B., Link, H., Randall, G., and McCoy, T.: Applicability of nacelle anemometer measurements for use in turbine power performance tests, Tech. rep., National Renewable Energy Lab., Golden, CO.(US), <https://www.nrel.gov/docs/fy02osti/32494.pdf> Accessed: 18/05/2023, 2002.

- Song, D., Yang, J., Liu, Y., Su, M., Liu, A., and Joo, Y. H.: Wind direction prediction for yaw control of wind turbines, *International Journal of Control, Automation and Systems*, 15, 1720–1728, <http://dx.doi.org/10.1007/s12555-017-0289-6>, 2017.
- 1235 Song, D., Yang, J., Fan, X., Liu, Y., Liu, A., Chen, G., and Joo, Y. H.: Maximum power extraction for wind turbines through a novel yaw control solution using predicted wind directions, *Energy conversion and management*, 157, 587–599, <https://doi.org/10.1016/j.enconman.2017.12.019>, 2018.
- Spencer, M., Stol, K., and Cater, J.: Predictive yaw control of a 5MW wind turbine model, in: 50th AIAA Aerospace Sciences Meeting including the New Horizons Forum and Aerospace Exposition, p. 1020, <https://doi.org/10.2514/6.2012-1020>, 2013.
- 1240 Spera, D. A.: Wind turbine technology, <https://www.osti.gov/biblio/6960578>, 1994.
- Starke, G. M., Stanfel, P., Meneveau, C., Gayme, D. F., and King, J.: Network based estimation of wind farm power and velocity data under changing wind direction, in: 2021 American Control Conference (ACC), pp. 1803–1810, IEEE, <https://doi.org/10.23919/ACC50511.2021.9483060>, 2021.
- 1245 Stieren, A., Gadde, S. N., and Stevens, R. J.: Modeling dynamic wind direction changes in large eddy simulations of wind farms, *Renewable Energy*, 170, 1342–1352, <https://doi.org/10.1016/j.renene.2021.02.018>, 2021.
- Storey, R., Cater, J., and Norris, S.: Large eddy simulation of turbine loading and performance in a wind farm, *Renewable Energy*, 95, 31–42, <https://doi.org/10.1016/j.renene.2016.03.067>, 2016.
- Stull, R. B.: An introduction to boundary layer meteorology, vol. 13, Springer Science & Business Media, 1988.
- 1250 Su, Z., Wang, J., Lu, H., and Zhao, G.: A new hybrid model optimized by an intelligent optimization algorithm for wind speed forecasting, *Energy conversion and management*, 85, 443–452, <https://doi.org/10.1016/j.enconman.2014.05.058>, 2014.
- Talbot, C., Bou-Zeid, E., and Smith, J.: Nested mesoscale large-eddy simulations with WRF: Performance in real test cases, *Journal of Hydrometeorology*, 13, 1421–1441, <https://doi.org/10.1175/JHM-D-11-048.1>, 2012.
- Tsioumas, E., Karakasis, N., Jabbour, N., and Mademlis, C.: Indirect estimation of the Yaw-Angle misalignment in a horizontal axis wind turbine, in: 2017 IEEE 11th International Symposium on Diagnostics for Electrical Machines, Power Electronics and Drives (SDEMPED), pp. 45–51, IEEE, <https://doi.org/10.1109/DEMPED.2017.8062332>, 2017.
- 1255 Van Der Hoek, D., Sinner, M., Simley, E., Pao, L., and van Wingerden, J.-W.: Estimation of the Ambient Wind Field From Wind Turbine Measurements Using Gaussian Process Regression, in: 2021 American Control Conference (ACC), pp. 558–563, IEEE, <https://doi.org/10.23919/ACC50511.2021.9483088>, 2021.
- 1260 Veers, P. S.: Three-dimensional wind simulation, Tech. rep., Sandia National Labs., Albuquerque, NM (USA), <https://www.osti.gov/biblio/6633902>, 1988.
- Vincent, C.: Mesoscale wind fluctuations over Danish waters, <https://www.osti.gov/etdeweb/biblio/1021047> Accessed:05/07/2022, 2010.
- Vincent, C., Giebel, G., Pinson, P., and Madsen, H.: Resolving nonstationary spectral information in wind speed time series using the Hilbert–Huang transform, *Journal of Applied Meteorology and Climatology*, 49, 253–267, <https://doi.org/10.1175/2009JAMC2058.1>, 2010.
- 1265 Wu, Y.-T. and Porté-Agel, F.: Large-eddy simulation of wind-turbine wakes: evaluation of turbine parametrisations, *Boundary-layer meteorology*, 138, 345–366, <https://doi.org/10.1007/s10546-010-9569-x>, 2011.
- Xin, W., Yanping, L., and Wei, T.: Modified hill climbing method for active yaw control in wind turbine, in: Proceedings of the 31st Chinese Control Conference, pp. 6677–6680, IEEE, <https://doi.org/10.1016/j.enconman.2017.12.019>, 2012.
- Yamartino, R. J.: A comparison of several “single-pass” estimators of the standard deviation of wind direction, *Journal of Applied Meteorology and Climatology*, 23, 1362–1366, [https://doi.org/10.1175/1520-0450\(1984\)023%3C1362:ACOSPE%3E2.0.CO;2](https://doi.org/10.1175/1520-0450(1984)023%3C1362:ACOSPE%3E2.0.CO;2), 1984.
- 1270

Yassin, K., Helms, A., Moreno, D., Kassem, H., Höning, L., and Lukassen, L. J.: Applying a Random Time Mapping to Mann modelled turbulence for the generation of intermittent wind fields, *Wind Energy Science Discussions*, 2021, 1–29, <https://doi.org/10.5194/wes-2021-139>, 2021.

Zahle, F. and Sørensen, N. N.: Characterization of the unsteady flow in the nacelle region of a modern wind turbine, *Wind Energy*, 14, 1275–283, <https://doi.org/10.1002/we.418>, 2011.

Zalkind, D. S. and Pao, L. Y.: The fatigue loading effects of yaw control for wind plants, in: 2016 American Control Conference (ACC), pp. 537–542, IEEE, <https://doi.org/10.1109/ACC.2016.7524969>, 2016.